DETECTING MONO CROPPING AND MIXED CROPPING FROM HIGH RESOLUTION IMAGES USING CURVELET TRANSFORM

MABOGUNJE OLUDARE OLA
FEBRUARY, 2017

SUPERVISORS:
Ms dr. Ir. Wietske Bijker
Dr. Valentyn Tolpekin

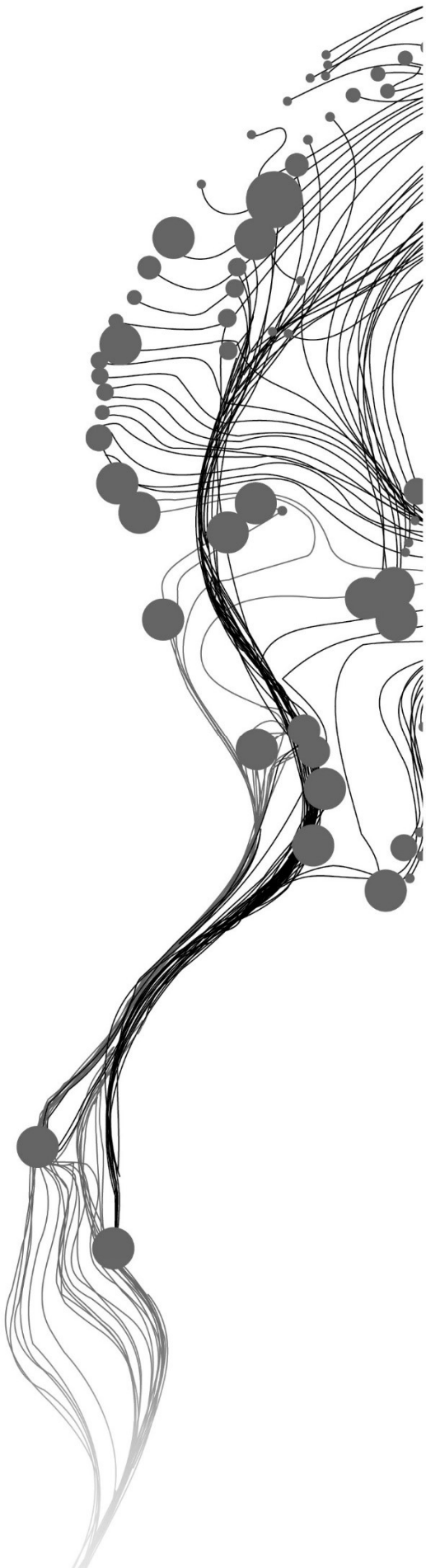

DETECTING MONO CROPPING AND MIXED CROPPING FROM HIGH RESOLUTION IMAGES USING CURVELET TRANSFORM

MABOGUNJE OLUDARE OLA
Enschede, The Netherlands, FEBRUARY, 2017

Thesis submitted to the Faculty of Geo-Information Science and Earth Observation of the University of Twente in partial fulfilment of the requirements for the degree of Master of Science in Geo-information Science and Earth Observation.
Specialization: Geoinformatics

SUPERVISORS:
Ms dr. ir. Wietske Bijker
Dr. Valentyn Tolpekin

THESIS ASSESSMENT BOARD:
Prof. dr. ir. A. Stein (Chair)
Dr. ir. T. A. Groen (External Examiner, University of Twente, ITC-NRS)

ABSTRACT

The economic activities of small farm holder are predominantly farming; the farming system practised is either planting one species of a crop (mono-cropping) or more than one species (mixed cropping) on the farmland. The study area is Kofa, Nigeria, the location is characterised by small farm holders practising mono-cropping and mixed cropping, the crops on the farmland have similar spectral characteristics hence the use of texture is necessary to distinguish them. This thesis work focuses on how to use curvelet transform to detect mono-cropping and mixed cropping system. The curvelet transform is applied to the image from the study area so as take advantage of different orientations provided at different resolution scales. The panchromatic image of Kofa, Nigeria which contains mono-cropping and mixed cropping fields was decomposed using curvelet transform. The image was decomposed using curvelet transform at scales 2, 3, 4, 5, 6 and 7, the orientations used at the second coarsest level for each is 8 and 16. The co-occurrence matrix of the curvelet coefficient was taken to investigate how well the detection can be improved. The classifier used is the support vector machine (SVM), the classification was done using the linear kernel of the SVM. The accuracy assessment was carried out using components of the confusion matrix.

The result obtained showed that the orientation at the second coarsest level is very important because it affects the performance of the classifier. The accuracies of detection of each crop vary per scale, some crops have a higher percentage of detection at one scale than at other scales. The highest accuracy is obtained at curvelet decomposition scale 4 with 8 orientations at the second coarsest level. When the co-occurrence matrix of the curvelet coefficient was included there was no overall improvement on the classification result.

ACKNOWLEDGEMENTS

I wish to express my gratitude and thanks to God for the wisdom, knowledge and understanding He has given me to be able to pursue this MSc. I wish to thank my supervisors Dr. Ir. Wietske Bijker and Dr. Valentyn Tolpekin for taking their time to thoroughly supervise this thesis, I appreciate the advice, patience and guidance shown to me during this research work.

I wish to express my gratitude to Joint Japan/World Bank Graduate Scholarship Program (JJ/WBGSP) (the "Scholarship Program") for awarding the scholarship for my MSc program. I say a very big thank you to the government of Japan for the full funding.

I wish to also thank my lecturers and course director for the lectures well delivered which reflected on my ability to carry out this research work. Also, I say thank you to my colleagues at the Faculty of Geo-Information Science and Earth Observation of the University of Twente (ITC) for the experience we had together. My appreciation also goes to the management of Centre for Satellite Technology Development (CSTD) and National Space Research and Development Agency (NASRDA) for their moral support and approval to embark on this program not forgetting, Dr. Muhammad Sanusi and Dr. Felix Ale for their encouragement to pursue an MSc. I thank the Redeemed Christian Church of God Enschede, Netherlands and World Evangelism Bible Church Abuja, Nigeria for their prayers and spiritual support.

My profound gratitude goes to my lovely wife Mrs. Adebimpe A. Mabogunje who prayed tirelessly for this dream of scholarship to come to reality, I love you and to my children Tioluwanimi Mabogunje, Oluwapamimo Mabogunje and Ibukunoluwa Mabogunje who continued to pray for my success, you are very much appreciated, I love you. To my precious mother Mrs J. Ola Mabogunje and my loved ones and well-wishers, I appreciate you all.

TABLE OF CONTENTS

LIST OF FIGURES

LIST OF TABLES

1. INTRODUCTION

1.1. Background

The type of crop on a piece of farmland has an impact on food security, agricultural development and resource management. Some societies base their income and living on agriculture, hence detecting the type of crops on a piece of farmland is very paramount to their economic development and well-being this is because the ability to monitor crops helps to improve crop production and thereby guaranty food security (Debats, Luo, Estes, Fuchs, & Caylor, 2016). Local farming systems are characterised by each farmer planting crops of several types, each type of crop has various subtypes which differ in features such as harvest time (Okigbo & Greenland, 1976), this method of planting various crops is practised for some reasons such as to mitigate inconsistent rainfall experienced annually and soil disparity (Stoop, 1986). Detecting the type of crops on a particular piece of farmland is useful in planning and making decisions, however, imprecise identification of some crops could occur, this could lead to taking wrong decisions. The Government needs to know the type of cropping systems on the farm to be able to effectively distribute fertilisers and insecticides. The Food and Agriculture Organization of the United Nations (FAO) needs to know about the cropping system to be able to assess the effectiveness and success of the second goal of the sustainable development goals. To be able to compensate farmers due to the loss incurred on their crops insurance companies need to have information about the crops on a farmland.

The term "cropping system" as used in this research means mono-cropping and mixed cropping. Mono-cropping as used is the practice of planting a single species of crop in a piece of farm field, while mixed cropping means cropping system which involves planting one species of crops in a row next to a different species on a row on the same piece of farm field or planting more than one species on the same row on a piece of farm field (no distinct row arrangement). The cropping system where crops are mixed has many benefits, for example, cocoa is mixed with food crop so as to take advantage of the fertile soil and receive protection from the food crop in terms of shade provided for the cacao seedlings (Duguma, Gockowski, & Bakala, 2001). Where there is high rainfall, cereals are usually planted with others cereals to take benefit of the rain (Stoop, 1987). It has been found that the type of cropping system practised could substantially improve the use of soil nutrients (Francis, 1989). When farmers mix crops, they get a high yield of the crop at maturity as opposed to when mono-cropping is practised, also mixed cropping maximises uptake of soil nutrient by crops when the crops have matured (Li et al., 2001). Zhang & Li (2003) observed that there was a greater substantial harvest when farmers mix wheat (wheat/maize and wheat/soybean intercropping systems) than when mono-cropping of wheat is practised. Seeking to further explore the benefit of mixed cropping, Christensen (2015) used land equivalent ratio to determine the efficiency of planting a variety of crops on a farmland and found out that there is an advantage to "land productivity and crop and market diversity" when planting a mixture of legumes and maize.

1.2. Problem Statement

A farmer knows what is planted on his/her farm but monitoring by the government will require the reports from farmers and government officials who go on site visits. This approach is very cumbersome due to logistics and the tendencies of error in communication due to the literacy level of the farmers. More so aggregation of farm fields amounts to thousands of acres at the district level, this makes sites visit time-consuming. There are problems associated with mixed cropping which might make it difficult for the

government to support the farmers if these problems are not well reported. Problems that could occur includes giving wrong information on the number of the acre of land planted with a certain type of crops, this makes it difficult for the government to estimate potential harvest in order to know how to support the farmers in terms of transportation and storage as might be needed.

Research shows that traditional pixel-based image analysis method leads to an imprecise identification of some crops due to inherent data characteristics such as "pixel heterogeneity, mixed pixels, spectral similarity, and crop pattern variability" (Peña-Barragán, Ngugi, Plant, & Six, 2011). These characteristics are linked to image resolution (spatial resolution and spectral resolution).

In the past detecting, several varieties of crops on a farmland using satellite images has been challenging due to the coarse spatial resolution of the satellite images used (Lu & Weng, 2007). The image spatial resolution has an impact on the accuracy of the image analysis method used, increasing the spatial resolution of images will contribute to an improved way of crop detection (Debats et al., 2016). The various crops on the piece of farmland may have similar spectral reflectance properties which could make it difficult to differentiate them using their reflectance properties alone. An alternative to the problem of spectral resolution is the spatial relationship of pixels of the image.

1.3. Research Identification

In a satellite image, a field containing mixed crops may be difficult to distinguish from a field with just one species of the crop because of spectral similarity among the crops. There is a need for using textures as a means for differentiation (Akar & Güngör, 2015), texture features have been used in relation to the resolution of the images (Kumar & Prema, 2015a). On high-resolution images, we see differences in the leaf size, plant spacing, and shape of the leaf. Curvelets have been used for texture features (Arivazhagan, Ganesan, & Kumar, 2006) however, its use in detecting mono-cropping and mixed cropping has not been found in the literature. Curvelet has been used with synthetic and non-synthetic images such as brodatz album (Liran Shen & Yin, 2007) and the MIT vision texture database (Vo & Oraintara, 2010). Texture analysis methods used in the past have similar characteristics of highlighting different aspects of texture (Livens, Scheunders, Wouwer, & Dyck, 1997).

Texture analysis methods like grey level co-occurrence matrix (GLCM) do not give a good performance for a noisy image while wavelet has the ability to filter noise (Patil & Lalitha, 2015). The use of transforms such as wavelet and curvelets has been used widely to improve feature detection, it was found that wavelet feature gives better accuracy for detecting features (Arivazhagan & Ganesan, 2003). The leaf area index of a crop has been estimated from multi-resolution data for barley using continuous wavelet. Hyperspectral data with spectral range 350nm – 1050nm of 10m, 15m, 20m, and 30m, were used in the study, the results obtained showed that using fused data is better than each of the multi-resolution data at different spatial scales (Dong et al., 2012). The use of wavelets and curvelets transforms an image into spatial and frequency domain, curvelets are an extension of wavelets.

Arivazhagan et al. (2006) discovered that curvelet features performed better than when wavelet features were used in feature detection. Sumana, Lu, & Zhang (2012) carried out an experiment on Brodatz texture and discovered that curvelet performed better than wavelet.

1.3.1. Research Objective

The main objective of this research work is to investigate and apply the use of curvelet transform in detecting mono-cropping and mixed cropping from high resolution satellite images.

Research sub-objectives are:

1. To investigate the use of curvelets in differentiating cropping systems from high resolution satellite images.
2. To investigate the effect of using curvelet co-occurrence matrix in improving the quality of cropping system detection.
3. To investigate the use of support vector machine in detecting cropping system.
4. To evaluate the accuracy of results.

1.3.2. Research Questions

1. What effect does using different curvelet decomposition resolution have on the quality of the output of the cropping system detection?
2. What curvelet co-occurrence matrix improves the result for detection algorithm?
3. What effect does support vector machine kernel parameter have on detecting cropping system?
4. What accuracy measures is best for the application?

1.4. Innovation Aimed At

The innovation aimed at is to make use of curvelet texture features for detecting mono-cropping and mixed cropping system from high resolution satellite image.

1.5. Outline of Thesis

Chapter 2 contains a review of related works on curvelets and feature detection. The chapter starts with a review of texture analysis from literature then it explores works of authors as it relates to extracting features and issues of rotational invariance of features. The work of authors using support vector machine for image classification is also reviewed.

Chapter 3 gives the description of the study area and the data used for this research work. In this chapter, the uniqueness of the study area is described paying particular attention to diverse crop rows as seen in the very high resolution satellite imagery. Also, the description of reference data and software used are stated here.

Chapter 4 details the methodology used in this research work. The use of curvelet is detailed in this chapter including decomposition and feature extraction. The chapter also details how the machine learning algorithm is incorporated into cropping system detection. It describes assessing the accuracy of the classification algorithm.

Chapter 5 presents the results. This chapter highlights the observation from the experiment on curvelet transform. Also, the result of machine learning algorithm is presented here including the accuracy assessment.

Chapter 6 presents the discussion on the results. This discusses the highlights from the experiment with an emphasis on characteristics of decomposition of curvelet and curvelet co-occurrence matrix. Also, the result of machine learning algorithm is discussed including the accuracy of classification result, highlighting the reliability of the thematic map.

Chapter 7 presents the summary of conclusion and recommendations. The outcome of the work done is iterated within the scope set. Also, recommendations for future work are given.

2. RELATED WORKS

2.1. Texture Analysis

Bovik, Clark, & Geisler (1990) defined image texture as "a local arrangement of image irradiances projected from a surface patch of perceptually homogeneous radiances". According to Nixon & Aguado (2012), textures are described so as to get measurements suitable for classification purpose, methods of texture description include structural, statistical, statistical geometric features (SGF), and local binary patterns. In the structural approach, a transform (such as Fourier transform, wavelet, curvelet) is applied to the entire image so as to expose its structure, frequency content is measured. In statistical methods such as co-occurrence matrix, the spatial relationships between brightness are measured. SGF method involves the use of statistics to describe the geometric features derived from images. In texture analysis, attributes that can be used for accomplishing tasks such as recognition, segmentation or discrimination are required (Bovik et al., 1990). Image texture can be said to be coarse or fine, coarse textures have mainly low spatial frequencies while fine textures mainly have a high spatial frequency (Haralick, 1979). The main spatial frequency in the textures that are different varies considerably hence this property can be used to differentiate them (Bovik et al., 1990). Based on the texture analysis method (frequency-based) texture can describe the texture as "an image pattern containing a repetitive structure that can be effectively characterised in a frequency domain" (Zou, Liu, Zhang, & Lu, 2013).

2.2. Feature Extraction

Features are "measurements, attributes or primitives derived from the patterns, that may be useful for their characterization"(Marques, 2001), Texture is a form of a feature. Busch & Boles (2002) carried out texture classification of 19 texture images from the "Brodatz album" using multiple wavelet algorithms (Haar and Biorthogonal), compared to single wavelet (Haar or Biorthogonal) methods for comparison. They observed that for simple energy features error rates are halved when multiple wavelets are employed implying that analysing image with more than one wavelet will provide additional information about the texture.

Lucieer & Van Der Werff (2007) classified high resolution satellite imagery using the texture features (spatial information) of the panchromatic band with spectral information of the multispectral band of a Quickbird image. The spatial resolution of the panchromatic band is 0.6 m and that of the multispectral bands is 2.4 m, four multispectral bands Blue, Green, Red, and Near Infra-Red were used. They expected the spatial characteristics of the land cover classes is contained in the panchromatic band while multispectral pixels provide spectral content. The Daubechies wavelet decomposition was applied to image block which is defined as containing 16 by 16 panchromatic pixels centred around a multispectral pixel. The texture is quantified using small-scale wavelet coefficients because they assumed that high frequency changes in pixel values depict the characteristic patterns. Entropy, standard deviation, skewness, kurtosis and energy were used as texture measure to capture the distribution of the wavelet. The research was used for vegetation classification, supervised fuzzy c-means classifier was used to classify the image of sub-Antarctic Macquarie Island. The purpose of the research was to improve classification, in comparison to a standard spectral classifier they obtained 5% increase in accuracy with the overall accuracy of 95.67% and Kappa coefficient of 0.94.

Kiani, Azimifar, & Kamgar (2010) extracted energy, entropy, inertia, local homogeneity and contrast features from Daubechies (Db4) wavelet transform. They discovered that the content and spatial orientations of images can be distinguished using wavelet transformation of digital images. Images of corn and weeds were acquired using a Canon Ixus digital camera in the farms of Shiraz University. They stored the digital images as a 24- bit colour images as RGB with a size of 1600×1200 pixels. The purpose was to find corn from an image containing corn and weeds. Artificial Neural Network (ANN) algorithm was used for the classification, the accuracy obtained is 98.8%.

Aware & Joshi (2015) extracted wavelet energy, entropy, inertia, contrast, and local homogeneity from Daubechies (Db4) wavelet. Images of sugarcane, onion and weeds were acquired using a Logitec C270 digital camera in Wai, Satara. They stored the digital images as a 24-bit colour image as RGB. The purpose of the research was to find weeds so that the coordinate of the weed is sent to a robot which moves its "manipulator" in the direction of the weed in order to spray herbicide on the weed. Artificial Neural Network (ANN) was used for classification, the researcher did not indicate the accuracy of the classification hence the success rate of detecting the weed for purpose of spraying herbicide cannot be established.

Arivazhagan, Ganesan, & Kumar (2006) decomposed images using discrete curvelet transform and extracted features using mean and standard deviation calculated from each of the sub-bands obtained. Candès, Demanet, Donoho, & Ying (2006) discovered that of the two fast discrete curvelet transforms (FDCTs) which are USFFT and wrapping, wrapping is faster. Dettori & Semler (2007) used wrapping algorithm, a spatial grid was used to translate curvelets at each scale and angle, it was assumed that the regular rectangular grid defines Cartesian curvelets. A 2D fast Fourier transform is applied to the image, a product of U_j is applied to each scale and angle. The result obtained is wrapped around the origin. The discrete curvelet coefficients are then obtained by applying the 2D inverse fast Fourier transform. Curvelet has also been used in the past for detecting edges in satellite high resolution images (Elhabiby, Elsharkawy, & El-sheimy, 2012).

2.3. Rotation Invariance

The word invariant is used to describe a situation in which an event or a phenomenon does not change when influenced by a variable, a function is said to be invariant if it remains unchanged after applying a particular transformation. For rotational invariant, the same feature with different orientation will be the same feature vector. Nixon & Aguado (2012) listed position, scale, and rotation as characteristics to be considered when extracting a texture invariance feature. This invariance required could depend on the application, most applications require position invariant whereas few applications require the scale invariant.

The problem of rotational invariance can be dealt with during feature extraction as can be seen in the work of most authors found in literature such as Manthalkar, Biswas, & Chatterji (2003), Zhi, Guizhong, Yang, & Junyong (2012), Jafari-Khouzani & Soltanian-Zadeh (2005), Riaz, Silva, Ribeiro, & Coimbra (2012). Another approach is to solve the problem during the classification, that is, during the machine learning stage (Hassan, Riaz, & Shaukat, 2014). Increased computational efficiency may be allocated to either feature extraction or machine learning stage or both, Manthalkar et al. (2003) suggested using both may improve the result.

Lahajnar & Kovačič (2003) approached the problem of rotation invariant classification of texture by using one rotation angle to train the samples while testing was done at other angles, it was discovered that the method performed well for difficult texture classifications.

Han & Ma (2007) achieved rotation invariance by taking a scale then summing up output at a different orientation in that scale. The image used is the Brodatz image which initially contained 112 textures, 1792 textures images were created by dividing image size of $512\ X\ 512$ into sixteen 128 non-overlapping images. The image was rotated into 16 equally spaced angles starting from zero with an increment of $\pi/16$. They used 3rd 4th 5th and 6th scale and the following orientations 4,5,6,7,8,9 at each scale. They discovered that when using one specific image type at one orientation to detect same image type rotated at different angles, 5 were retrieved correctly using conventional Gabor while all the rotated images were retrieved using their rotation-invariant Gabor features as shown in Figure 2-1, the image in the top-left is used as the query image

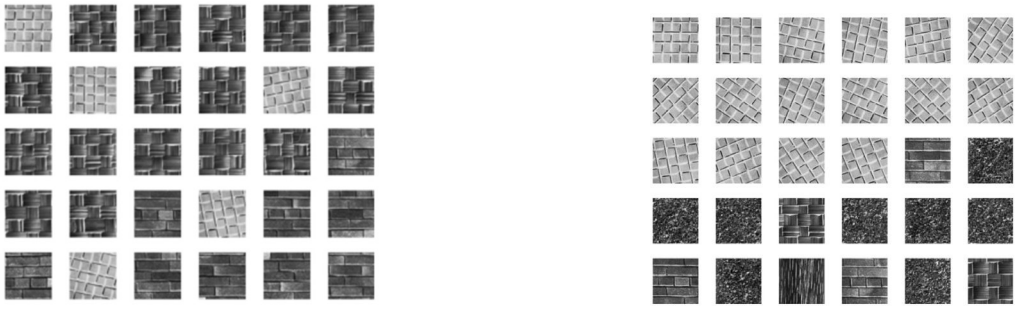

a. conventional Gabor representation b. rotation-invariant Gabor representation

Figure 2-1. Result of retrieving texture image using Gabor features. Source: Han & Ma (2007)

Livens et al. (1996) used rotational invariant features to reduce feature dimension and discovered that after wavelet decomposition, adding the energy of the features present in each scale leaves out information about the orientation, which makes the direction of the energy irrelevant. The image used was a scanned corrosion photograph of size 128 by 128 pixels with 64 grey levels, wavelet decomposition was done using 9 tap bispline wavelets.

When dealing with rotational invariance in some images, some sub-bands (rotational angles) are symmetric, for example, sub-bands 45° and 135° (Kingsbury, 2006) give similar frequency response. Islam, Zhang, & Lu (2009) proposed rearranging curvelet features to make curvelet rotational invariant. Rotation invariance has also been considered in the use of curvelet by some authors (Zhang, Islam, Lu, & Sumana 2012; Gómez & Romero 2011; Cavusoglu 2014).

2.4. Image Classification

Haykin (2001) described a filter as a tool used to extract information, it does filtering, smoothing, and prediction. Support vector machine (SVM) is an example of a filter (classifier). SVM is a non-parametric classifier, for a non-parametric classifier, class separability is not calculated using statistical parameters (Lu & Weng, 2007). SVM does not suffer from the curse-of-dimensionality because of the quadratic programming method employed (Haykin, 2001). SVM is a linear classifier (Richards, 2013), it uses kernel such as linear kernel (Chen, Wang, Wu, Jiang, & Li, 2016), radial basis function kernel (Rokni, Ahmad, Solaimani, & Hazini, 2015) and Fisher kernel (Kaur & Pooja, 2015).

SVM classifier has proven to be successful in range of applications such as crop type classification (Akhtar, Nazir, & Khan, 2012), plant disease classification (Pujari, Yakkundimath, & Byadgi, 2016), weed detection classification using texture features extracted from wavelet transform (Kumar & Prema, 2015b), face

recognition (Liang, Gong, Pan, Li, & Hu, 2005), and face detection (Serrano, de Diego, Conde, & Cabello, 2010). SVM has been used in classifying feature extracted from wavelet transform (S. Li & Shawe-Taylor, 2005), when used with Gabor wavelets it can be optimised to provide better performance (Shen & Ji, 2009). The use of SVM with curvelet is in the work of Prema & Murugan (2016).

In image classification there are errors associated with the results, these errors could be quite catastrophic, the consequence of the errors largely depends on the application (DeFries & Los, 1999), it is important to quantify these error because a reliable map could be useful in safety critical scenario (Congalton & Green, 2009). Foody (2002) described the value of a map to be based on how accurate the classification is. Accuracy assessment can be described as an approach which involves checking a map with a reference data (Campbell & Wynne, 2011). Congalton's 1994 study (as cited in Foody, 2002) described the approached used in measuring accuracy these methods range from the subjective method described as the visual appraisal to objective methods which includes areal extent accuracy, overall accuracy and the confusion matrix. Confusion matrix has wide use in the scientific community for assessing the accuracy of a classification map (Canters, 1997). Kappa coefficient has been found to be problematic in assessing the accuracy of classification map (Pontius & Millones, 2011).

3. DATA

3.1. Study Area

The study area is Kofa in Kano state, located at 11°33'08.9"N, 8°16'06.6"E in the Northern part of Nigeria West Africa (Figure 3-1). The farming system practised is predominantly mixed cropping, it is made up of small farm holders and aggregation of farmlands. The single variety of crop types is sorghum, soybeans, maize, rice and mixed cropping of onions and pepper, sorghum and soybeans, and also soybeans and sorghum.

3.2. Imagery and Reference Data

3.2.1. Very High Resolution Satellite Image

The image used in this research work is Worldview-3 very high resolution satellite images of the study area (Kofa, Nigeria) containing mono cropping and mixed cropping system. The date of acquisition of the Worldview-3 image is 25th September 2015. The ground sampling distance (GSD) of the panchromatic band used is 0.5 m.

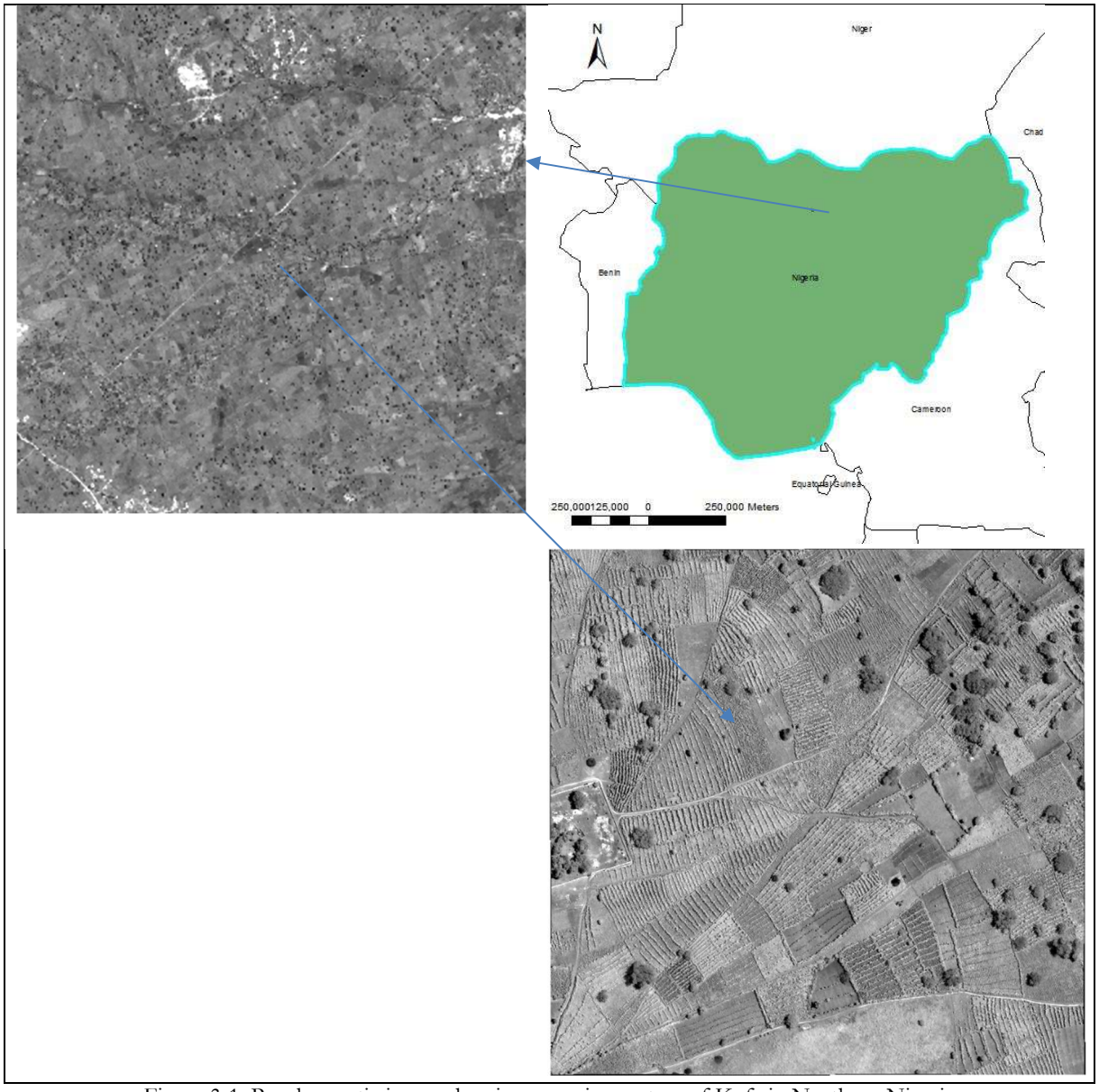

Figure 3-1. Panchromatic image showing cropping system of Kofa in Northern Nigeria

3.2.2. Reference Data

The reference datasets used are based on field photos acquired by STARS project and manually digitised polygons of farm fields of the 0.5m panchromatic image of Kofa acquired on 25th September 2015.

3.3. Software

The software used are:

1. Erdas Imagine 2015 was used for sub-setting
2. MATLAB R2016b was used for curvelet analysis
3. R was used for graphic analysis and statistical computation (R Core Team, 2016).
4. Envi Classic 5.3 was used for feature extraction.
5. ArcMap 10.4.1 was used for field extraction.

4. METHODOLOGY

4.1. Method Adopted

The method used in achieving the objective of this research is extracting texture features from image decomposed using curvelet transform for the purpose of detecting cropping system from high-resolution satellite images. Texture analysis has been approached using two main perspectives, structural and statistical. Structural perspective describes the texture as texture elements ("texels") made up of some regular or repeated association (particular spatial relationship). The statistical approach quantitatively measures the arrangement in a region. The statistical approach is used more often in practice and is more general and easier to compute (Shapiro & Stockman, 2001). The steps used to accomplish the method is as shown in Figure 4-1.

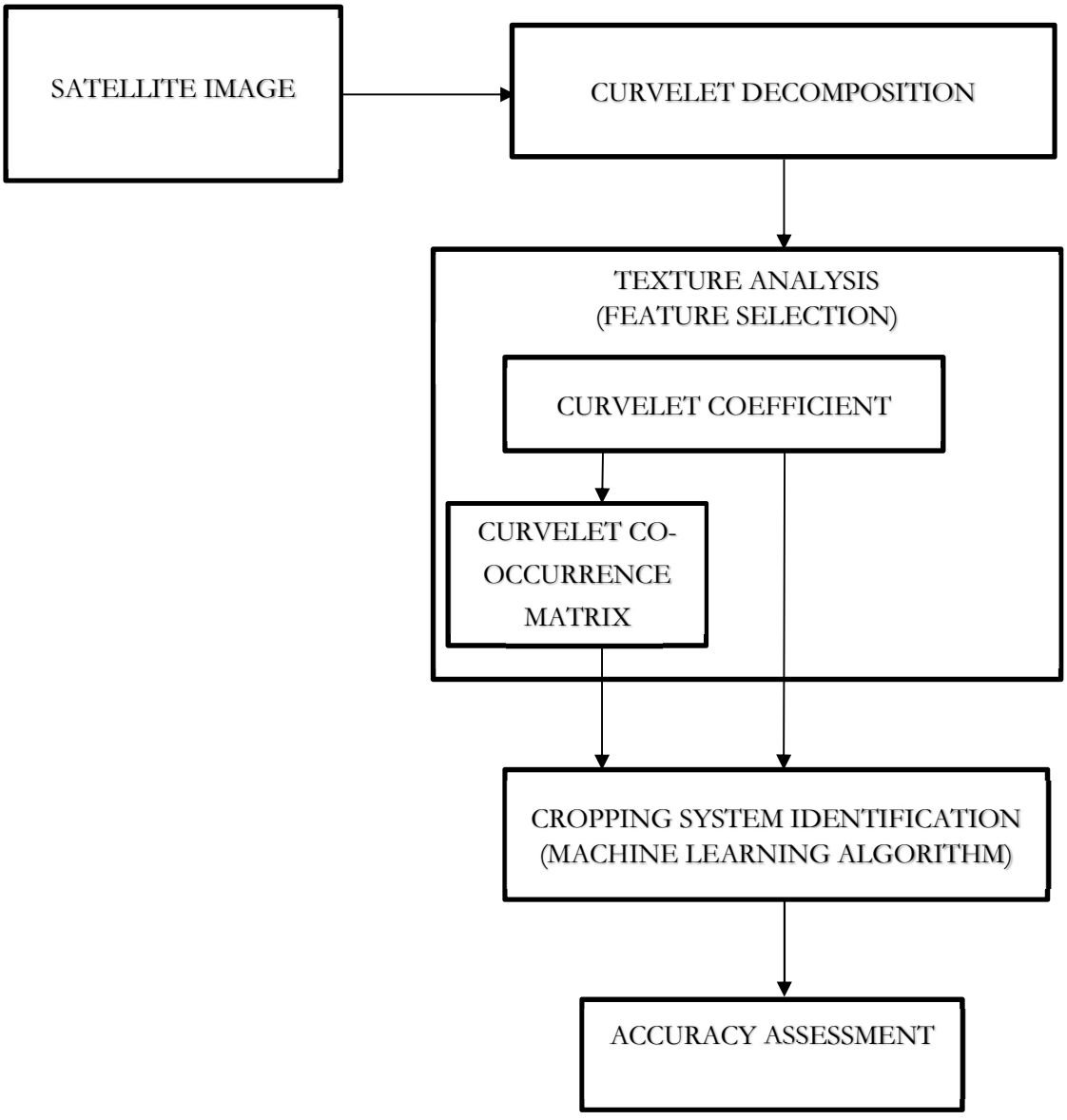

Figure 4-1. Flow diagram showing the method used

4.2. Curvelet Transform

Curvelet is an extension of wavelets, wavelets are useful for analysis at different resolution(scales) and allow decomposition in space and frequency simultaneously (Nixon & Aguado, 2012). Wavelet analysis decomposes images into a single low-pass image and multiple high-pass images, the decomposition is repeated using the low-pass image (Han & Ma, 2007), while curvelet decomposes at a different scale and orientation. Curvelet transform is chosen for this thesis work as opposed to wavelets because of its directional properties, it is efficient in representing edges and other singularities along curves. The implementation of curvelet chosen is the second generation fast discrete curvelet transform which uses wrapping.

Symbol	Meaning
u	spatial frequency along the x axis of the original image
v	spatial frequency along the y axis of the original image
$R(u,v)$	the real part of the image Fourier transform
$I(u,v)$	the imaginary part of the image Fourier transform
$\|H(u,v)\|$	amplitude of the sine and cosine wave
θ	phase of the sine and cosine wave
$h(x,y)$	image to be transformed
MN	Size of image
j	scale
x,y	spatial- domain variables
ω	frequency- domain variable
r and θ	polar coordinates in the frequency-domain
$\vartheta_{j,l}$	wrapping output
l	Rotation l
T	product of the discrete localizing window and Fourier samples
W	Wrapped window
n_1, n_2	pixel indices
$f[n_1,n_2]$	Fourier samples
$\tilde{\mathrm{U}}_{j,l}$	discrete localizing window

Table 4-1. Parameters for fast discrete curvelet transform

4.2.1. Frequency Analysis

The image to be decomposed is subset into M columns by N rows. The spatial frequency which is the rate at which the pixel intensities change in the image is obtained after applying Fourier transform. The magnitude of the different frequency components in the image is obtained using the frequency domain. The discrete Fourier transform is used instead of the ordinary Fourier transform (Equation 4-1) because digital image is used. The magnitude (Equation 4-2) is used to represent the image.

$$H(u,v) = \frac{1}{MN}\sum_{x=0}^{M-1}\sum_{y=0}^{N-1} h(x,y)e^{-j2\pi\left(\frac{ux}{M}+\frac{vy}{N}\right)} \quad (4\text{-}1)$$

$$|H(u,v)| = \sqrt{R^2(u,v) + I^2(u,v)} \quad (4\text{-}2)$$

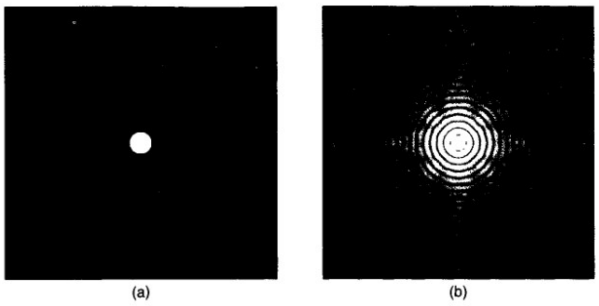

Figure 4-2. Fourier transform of a spot: (a) original image; (b) Fourier transform. Source: Crane (1997)

In an image transform, the frequency and pixel location are interdependent, using a spot when the Fourier transform is obtained far away from the origin it has a higher spatial frequency (Figure 4-2).

The computational complexity of discrete Fourier transform (FT) is high, this led to the use of Fast Fourier Transform (FFT). The use of FFT for data transformation in frequency domain requires the use of image with dimension powers of 2 because of the algorithm of FFT recursively divides the data into 2.

In wavelets, the Fourier transform is generalised by using a basis that represents both location and spatial frequency. Directional wavelets have basis functions that are also localised in orientation included. For curvelet the degree of localisation in orientation varies with scale. Candès et al. (2006) described curvelet transform as a multiscale pyramid that has many directions and positions at each length scale, while the fine scales are made up of needle-shaped elements (Figure 4-3). They exhibit parabolic scaling relation which states that at each scale, each element is put in a case which is aligned along a support of length $2^{-j/2}$ and width 2^{-j} (Equation 4-5). The second generation curvelet transform uses fast discrete curvelet transforms (FDCTs), it is implemented using two approaches the first approach uses unequally-spaced fast Fourier transforms (USFFT) and the second approach uses wrapping of specially selected Fourier samples. The spatial grid used to translate curvelets at each scale and angle is a differentiating factor of the two approach, however, the output of the two gives a table of digital curvelet coefficients indexed by a scale parameter, an orientation parameter, and a spatial location parameter. It is faster to perform 2-dimensional FT in the frequency domain than to perform convolution in the spatial domain. The description of the curvelet transform parameters is shown in Table 4-1

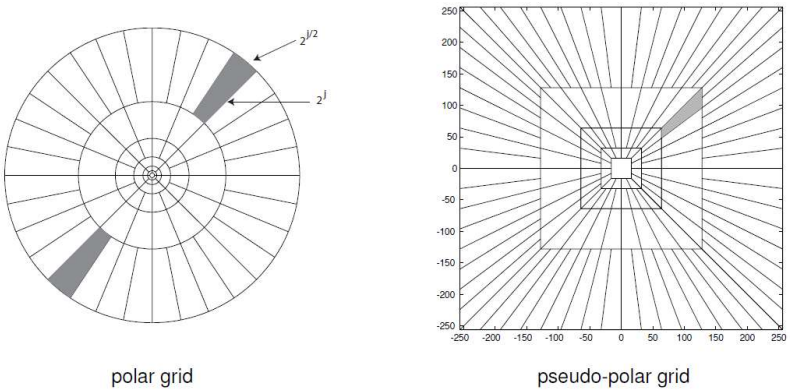

Figure 4-3. Basic digital tiling showing shaded region of wedge at scale 4 orientation 1.
Source: Candès et al. (2006)

The image to be decomposed is input into the FDCT using wrapping the output gives curvelet coefficient (CM). The following section gives the details of each step needed to fully decompose the image.

$$T = \tilde{\mathrm{U}}_{j,l}\,[n_1, n_2] f[n_1, n_2] \tag{4-3}$$

$$\vartheta_{j,l}\,[n_1, n_2] = W(\tilde{\mathrm{U}}_{j,l}\, f)[n_1, n_2] \tag{4-4}$$

$$2^{-j/2} \approx 2^{-j} \tag{4-5}$$

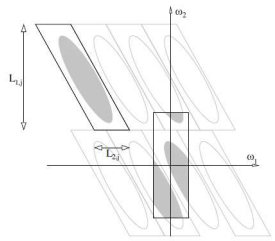

Figure 4-4 Wrapping data in a parallelogram to rectangular. Source: Candès et al. (2006)

The 2D FFT is applied to the image, the output is Fourier samples $f[n_1, n_2]$ in the range $-n/2 \leq n_1, n_2 < n/2$. Resampling is done using a Cartesian grid, at each scale j and angle ℓ by multiplying $\tilde{\mathrm{U}}_{j,l}\,[n_1, n_2]$ by $f[n_1, n_2]$. This product is now wrapped around the origin, the result is $\vartheta_{j,\ell}$,. Figure 4-4 shows the how wrapping of the data is done here, the range of n_1 and n_2 changes to $0 \leq n_1 < L_{i,j}$ and $0 \leq n_2 < L_{2,j}$, such that angle is within$(-\pi/4\,, \pi/4\,)$, at the origin the rectangle is centrally placed, the parallelogram holds the frequency support of the curvelet and using periodization the other parallelograms are duplicated. The ellipse (Fourier samples) in the parallelogram is wrapped into the rectangle. Finally the inverse 2D FFT is applied to each $\vartheta_{j,\ell}$, to get the discrete coefficients C $_{(j,\,\ell\,,\,k)}$. The curvelet parameters are scale, location, and orientation parameters

To make curvelet directional, each scale is divide into constant number such as 8 or 16 angles. Each level is further subdivided into a region shaped like a trapezoid known as angular wedges. The elements of the coefficient matrix can be identified by scale and location at the orientation. The value of the rotation doubles at the next two scale.

The notation used in this thesis to describe decomposition is as follows X is scale of decomposition, A represents the number of rotations, S is the sub band and R represents the rotation. To describe a coefficient $Xn\_An\_Sn\_Rn$ is used which means curvelet coefficient of Xn decomposition scale and An second coarsest angles at sub band Sn and orientation Rn. Each scale is divided into $16\ X\ 2^{\lceil (j-1/2) \rceil}$ wedges

4.2.2. Curvelet Coefficient Feature

Each coefficient belongs to a scale 2^{-j} and is located at a rotation angle. The equally spaced sequence of rotation angles is such that $0 \leq \theta l < 2\pi$, spacing between consecutive angles depends on scale see Figure 4-2

$$\theta_l = 2\pi \cdot 2^{-\lfloor j/2 \rfloor} l \tag{4-6}$$

4.2.3. Curvelet Co-occurrence Matrix (CCM) Feature

Haralick (1979) defined second order statistical feature of which eight are used in this project work. The computation of these texture features which were initially defined for computing grey level $(P_{i,j})$ in the cell $(i,j)th$ has been adapted for curvelet coefficient in this project work hence $P_{i,j}$ is the curvelet coefficient in the cell $(i,j)th$ of the matrix MN, N is the number of rows. The eight second order statistics of curvelet co-occurrence matrix (CCM) computed with Equation 4-7 to Equation 4-14 are listed below. The distance of neighbouring pixel considered in this project work is for distance d=1 and window size $3x3$ is used.

CCM Mean

$$\mu_x = \sum_{i=0}^{N-1} i\left(P_{i,j}\right) \ , \ \mu_y = \sum_{j=0}^{N-1} j\left(P_{i,j}\right) \tag{4-7}$$

CCM Contrast

$$c = \sum_{n=0}^{N-1} n^2 \left\{ \sum_{\substack{i=1 \\ |i-j|=n}}^{N} \sum_{j=1}^{N} \left(P_{i,j}\right) \right\} \tag{4-8}$$

CCM Dissimilarity

$$D = \sum_{n=1}^{N-1} n \left\{ \sum_{\substack{i=1 \\ |i-j|=n}}^{N} \sum_{j=1}^{N} \left(P_{i,j}\right)^2 \right\} \tag{4-9}$$

CCM Homogeneity

$$H = \sum_i \sum_j \frac{P_{i,j}}{1+(i-j)^2} \tag{4-10}$$

CCM Variance

$$\delta^2 = \sum_i \sum_j (i-u)^2 P_{i,j} \tag{4-11}$$

CCM Correlation

$$Cl = \frac{\sum_i \sum_j (ij) P_{i,j} - \mu_x \mu_y}{\delta_x \delta_y} \tag{4-12}$$

CCM Second moment

$$Sm = \sum_i \sum_j P_{i,j}^2 \tag{4-13}$$

CCM Entropy

$$E = -\sum_i \sum_j \left(P_{i,j}\right) log\left(P_{i,j}\right) \tag{4-14}$$

4.3. Support Vector Machine (SVM) Classification

Support vector machine is used to detect the cropping system. The choice of this is based on the fact that the feature space of the output from the curvelet decomposition is large and others attributes earlier identified from literature such as SVM being a non-parametric classifier. The SVM works by making use of separating hyperplane which is the decision boundary, the separating hyperplane is created taken into consideration that the separation margin between two class A and class B samples is maximised characteristics of the training samples such as the distribution of feature space is also taken into account.

In this project work the two import choices made in applying the SVM classifier is training the classifier and choice of kernel parameters. The training was done so that the optimal hyperplane can be achieved. The data set used for training and testing are split into two disjoint set (hold out method). The data is not linearly separable thereby creating noise in the training set, this makes it difficult to achieve optimal result, which results in high error in classification. The solution to the problem is tuning parameters, two type of kernel were used the linear and radial basis function (RBF) and the regularization parameter C was varied. The regularisation parameter C is used to control penalty associated to the errors, the value of C is chosen so that it is not too small thereby causing a lot of error to be allowed, if this happens the discriminant function will not fit the data very well. Likewise, if C is too large overfitting will occur which leads to poor generalisation.

SVM is a binary classifier, this project work uses the adaptation to multiclass system which is one-against-one. In one-against-one all the binary sub classifiers are fitted then the correct class is chosen by voting rule.

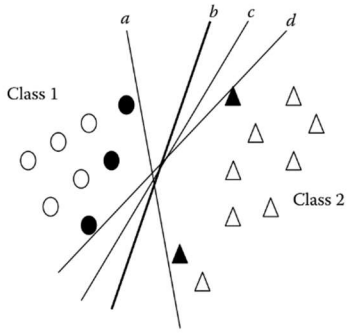

Figure 4-5 SVM with hyperplane separates the two classes with the maximal margin. Source: Tso & Mather (2009)

In Figure 4-6 the line b is the hyperplane which divides the two classes with the maximal margin. When there are x_i features and y_i labels of information class for training instance i, the training data set is $\{ x_i, y_i \}$ where $i = 1, \dots, n \; y_i \in \{A, B\}$ and $x_i \in R^d$, A denotes class A and B denotes class B. The SVM classifier tries to create the best hyperplane (Figure 4-6) which divides the two classes such that the largest

possible margin from training data point in classes A to the hyperplane and that of class B to the hyperplane should be created.

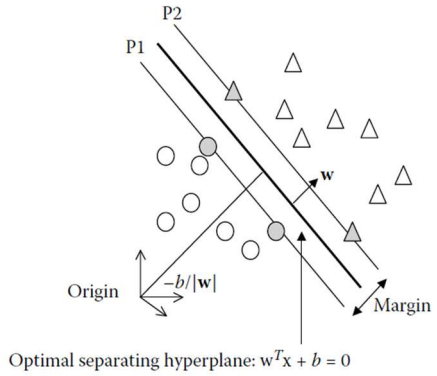

Figure 4-6. Optimal hyperplane separating two classes. Source: Tso & Mather (2009)

4.4. Accuracy Assessment

The confusion matrix is considered sufficient for this research; this choice is made based on wide acceptability in remote sensing and to enable easy comparison of the results with other work. Kappa coefficient was not used due to its complexity and other problems identified in literature.

The confusion matrix (Figure 4-7) was used to display classification accuracy and errors, then the results were examined to locate interclass confusion so as to improve the classification further, curvelet co-occurrence matrix feature was also was used to provide features which was used to investigate how well the classes can be distinguished so as to reduce this confusion.

The elements Z_{ij} of the confusion matrix are used to derive different accuracy measures. In this study based on the uses identified, components of the confusion matrix used are listed below. These measures were used to examine the trend of class distribution compared to reference data set.

- Overall Accuracy.
- User Accuracy.
- Producers Accuracy.

		ACTUAL CLASS			
		1	2	3	4
PREDICTED CLASS	1	Z_{11}	Z_{12}	Z_{13}	Z_{14}
	2	Z_{21}	Z_{22}	Z_{23}	Z_{24}
	3	Z_{31}	Z_{32}	Z_{33}	Z_{34}
	4	Z_{41}	Z_{42}	Z_{43}	Z_{44}

Figure 4-7. Confusion matrix showing arrangement of elements

5. RESULT

5.1. Curvelet Transform

The decomposition of the image using Daubechies' wavelet (Daubechies, 1992) and curvelet is shown in Figure 5-1, this shows that curvelet could model the curves of the feature better than Daubechies' wavelet. Curvelet has the ability to model curve discontinuity well. To describe scale and orientations, $Xn\_An\_Sn\_Rn$ notation is used, where Xn is decomposition at scale n, An is number of orientations at the second coarsest level, Sn is sub scale (sub band) n and Rn is orientation n, for example X4_A8_S2_R1 is coefficient obtained by decomposition Scale 4 and 8 number of orientations located at sub-scale 2 orientation 1, S2_R1 means coefficient at sub-scale 2 orientation 1, similarly X4_A8 means decomposition at scale 4 and orientation 8.

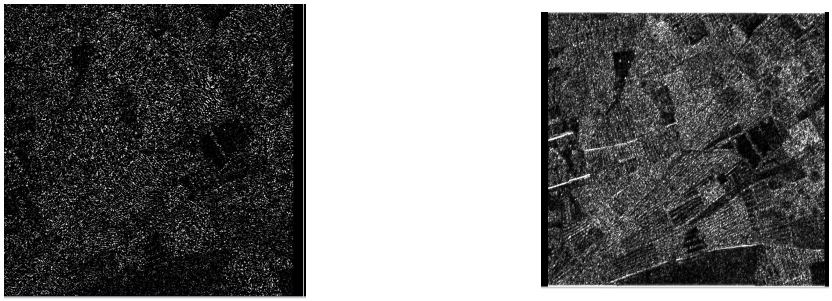

a. b.

Figure 5-1. Coefficient of decomposed image of farm field a. Daubechies' diagonal coefficient b. Curvelet S2_R3 coefficient

Figure 5-1 shows the coefficient obtained by decomposing the panchromatic image using Daubechies and curvelet transform. In the Daubechies output the farm fields are not well defined while in curvelet transform the farm fields are better modelled and the edges are well preserved and emphasised. Exploring the directional ability of the curvelet further, the decomposition was done at scale 2, 3,4,5,6, and 7 (X2_X7) using second coarsest level orientations 8 and 16. The choice of maximum scale is based on the computation suggested in literature, moreover it was found out that when the scale is beyond the recommended level some coefficients gives undefined results. The orientation 8 was used because it was found suitable for analysis, at 2nd level each angle gives 45º and at the highest scale of 7 each is 5.6 º while at orientation 16 the 7th scale gives 2.82 º degrees. The software Curvelab (2016) of 2nd generation curvelet implementation is used in decomposing the images. The study area contains similar crops that are planted in different orientations, it is expected that since the similar crop features are the same they are to be detected as similar when oriented differently. To achieve this, features in all orientations of the sub scale except sub scale 1 feature are considered from the output of curvelet decomposition. Sub scale 1 (coarsest scale) has only one orientation, it is not used for analysis in this thesis work. The total number of features per scale can be seen in Table 5-1, counting the number of features without counting sub scale 1 gives a total of 8 features for decomposition at X2_A8, decomposition at X7_A8 gives a total of 168 features, when the orientation is doubled the number of features also doubles.

Total number of features in decomposition scales							
Angles	j=1	j=2	j=3	j=4	j=5	j=6	j=7
8	1	8	16	16	32	32	64
16	1	16	32	32	64	64	128

Table 5-1. Number of features at various decomposition scales

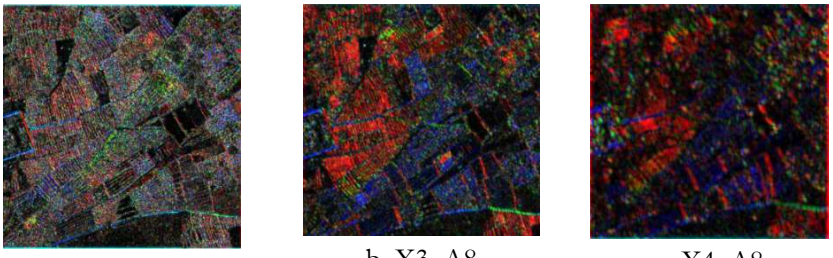

a. X2_A8 b. X3_A8 c. X4_A8

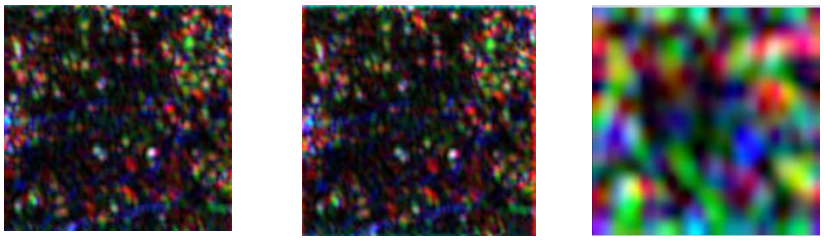

d. X5_A8 e. X6_A8 f. X7_A8

Figure 5-2. RGB combination of scales, band combination S2_R3,S2_R2,S3_R1

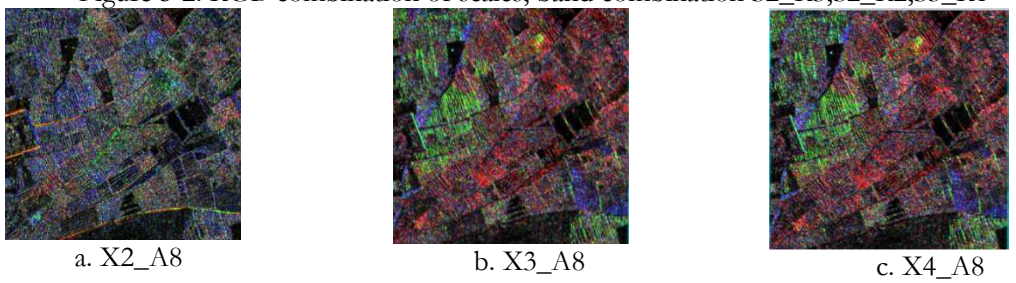

a. X2_A8 b. X3_A8 c. X4_A8

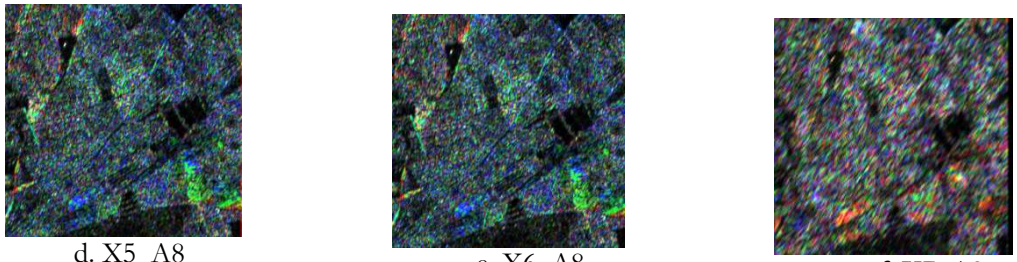

d. X5_A8 e. X6_A8 f. X7_A8

Figure 5-3 RGB combination of scales, band combination is 4th ,5th ,2nd element of first sub scale

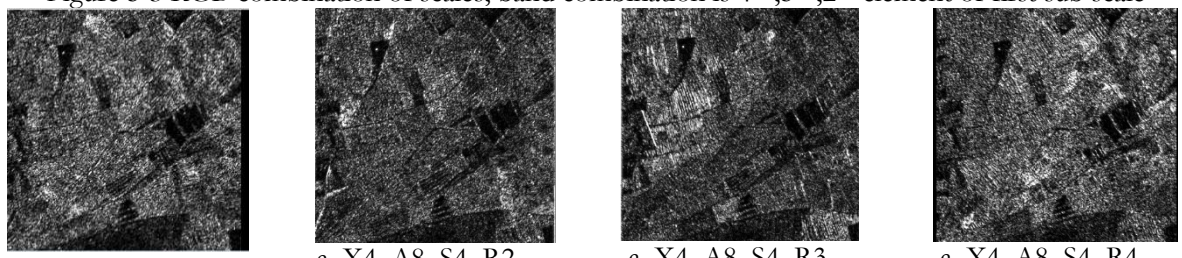

a. X4_A8_S4_R1 a. X4_A8_S4_R2 a. X4_A8_S4_R3 a. X4_A8_S4_R4

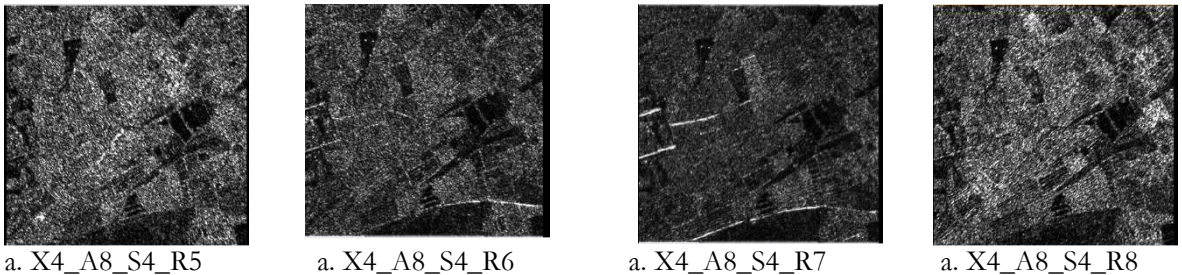

a. X4_A8_S4_R5 a. X4_A8_S4_R6 a. X4_A8_S4_R7 a. X4_A8_S4_R8

Figure 5-4. Curvelet of first 8 elements of X4_R8.

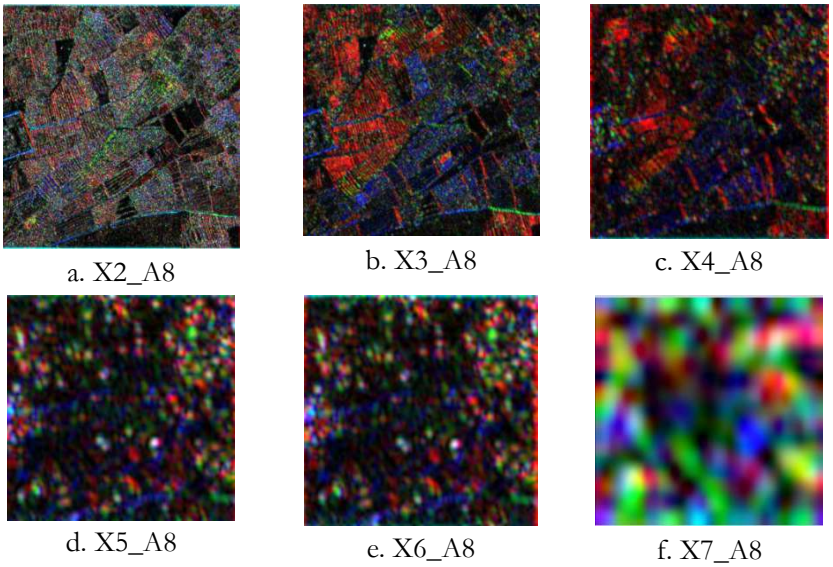

a. X2_A8 b. X3_A8 c. X4_A8

d. X5_A8 e. X6_A8 f. X7_A8

Figure 5-2 shows the RGB of second coarsest level of scale X2 to X7, the band combination is the 3 last band of each scale. From the figure the farm fields become less distinguishable. This is as a result of aggregation caused at sub band 2 as decomposition scale increases from X2 to X7. As the scale increases the crop rows are no longer visible at scale X7 it becomes difficult to see farm fields.

Figure 5-3 shows the RGB of the curvelet coefficient at orientation 4, 3, 2, of the finest sub scale of X2 to X7. At this sub scale the fields can be located.

When considering the curvelet coefficient in different directions located at one scale, for example decomposition at X4_8 (Figure 5-4) each field behaves differently, for example a field can have its edges preserved in more than one orientation this makes it more distinguishable at those orientations. The orientation in which a farm field has a high frequency means the crop has a good distinguishing properties which will be used by the classifier to separate the crops.

The effect of the scale and the orientation in distinguish the cropping system is much visible from the classification map.

5.2. Support Vector Machine (SVM) Classification

The result of one-against-one approach which is offered by the interface to libsvm in package e1071 (Meyer, Dimitriadou, Hornik, Weingessel, & Leisch, 2015) of R software is presented here. To classify the features, supervised classification is carried out, classes are defined using training samples from the fields listed below

- Sorghum
- Soybeans
- Maize
- Rice
- Onions and Pepper
- Sorghum and Soybeans
- Soybeans and Sorghum

The class Sorghum and Soybeans represents field with sorghum as the predominant crop while soybeans and sorghum represent field with predominantly sorghum. The Daubechies' wavelet features used were the vertical, horizontal and diagonal features of two level decomposition, the output was not explored further

because the classes could not be distinguished by the classifier. Figure 5-5 shows the SVM classification using the CCM decomposed a. scale 3 and 8 orientation b. scale 3 and 16 orientation c. scale 4 and 8 orientations d. scale 4 and 16 orientations. The confusion matrix of the linear SVM classification are shown in Table 5-3 to Table 5-7.

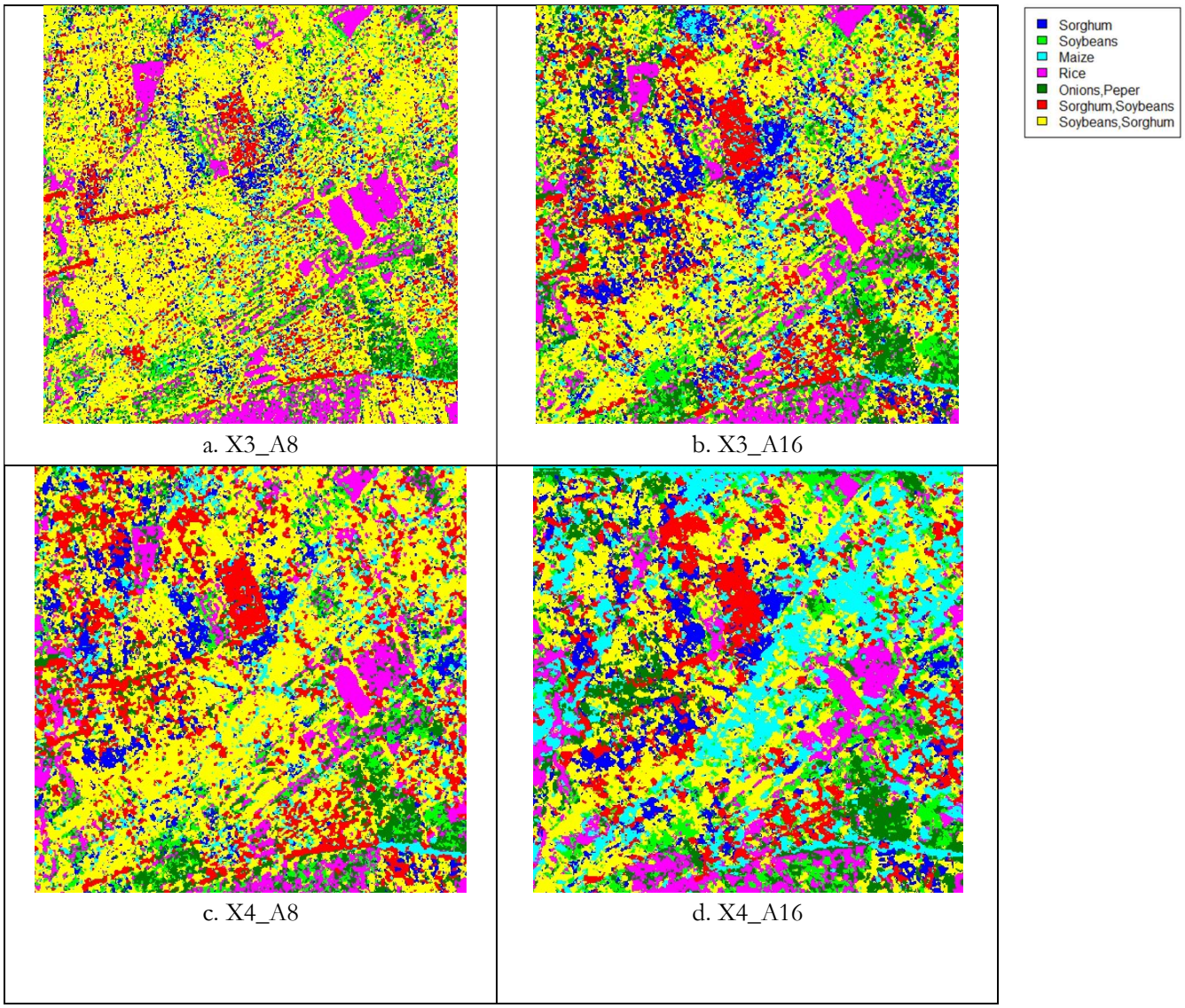

a. X3_A8

b. X3_A16

c. X4_A8

d. X4_A16

Figure 5-5 SVM classification map of X3 and X4 at orientations 8 and 16

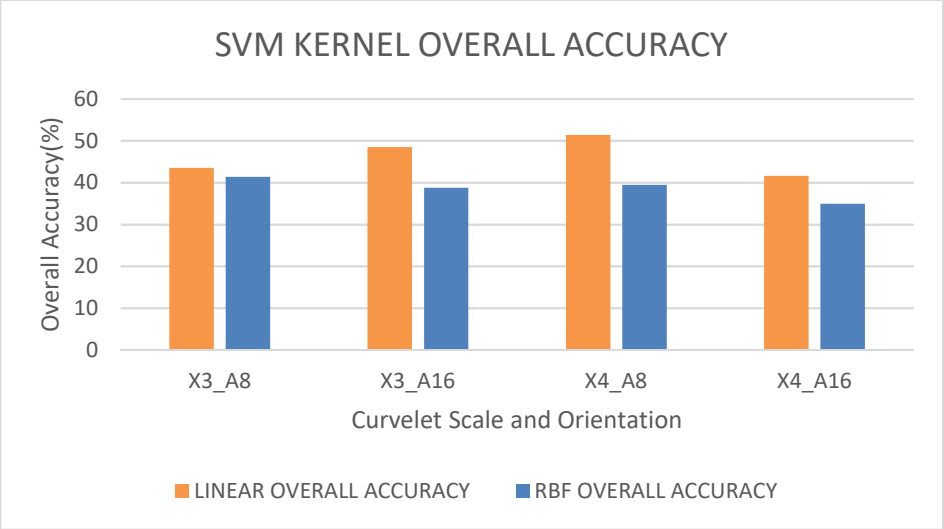

Figure 5-6. Graph of overall accuracy using Linear and RBF kernel of SVM

The result of SVM classification is shown in the map in Figure 5-5, it shows mixed cropping of sorghum and soybeans are predominant in the first 3 maps. From the map, it is easier to distinguish fields in low scales than when the scale is increased. The three decompositions X3_A8, X3_A16 and X6_A8 looks similar in their appearance, X4_A16 is not close to what is expected as mono-cropping of maize has taken over the place of mixed cropping of sorghum and soybeans. Maize is highly misclassified. The result of the using co-occurrence matrix to improve the accuracy is shown in Table 5-2, the overall accuracies shows only the mean CCM is slightly greater than the CCM, all other co-occurrence feature did not improve the accuracy

To improve the classification further RBF kernel of the SVM was used. The RBF kernel was explored using parameters of cost 10 and gamma 0.5, the parameters were chosen arbitrarily, the result of overall accuracy is shown in Figure 5-6. Most of the classes were not identified; the result was not investigated further. This is likely due to the fact that the parameters were not tuned to obtain the optimal result. The graph shows the overall accuracy of using linear and RBF kernel, it shows that Linear SVM outperforms the RBF SVM. The overall accuracy is not substantial enough to correctly compare the classification of both maps, looking at the performance of each classes could have given better insight into the reason for the performance but the most classes were not classified.

Feature	X3_A8	X3_A16	X4_A8	X4_X16
CCM	43.6	48.5	51.4	41.6
Mean CCM	44.6	49.4	52.8	40.5
Contrast CCM	41.6	42.6	43.6	40.6
Dissimilarity CCM	41.4	41.4	42.8	41.2
Homogeneity CCM	39.2	39.7	41.4	42.0
Variance CCM	43.0	42.8	43.3	42.1
Correlation CCM	34.8	37.7	36.6	37.6
Secondmoment CCM	43.3	42.4	42.1	40.2
Entropy CCM	39.5	42.9	42.0	40.3

Table 5-2. Overall accuracy of linear SVM classification of co-occurrence curvelet coefficient

Table 5-2 shows the overall accuracy of linear SVM classification of co-occurrence curvelet coefficient decomposition (CCM) at different scales and different angles of orientation. The co-occurrence matrix does not generally improve the overall accuracy except a slight increase when the mean is taken at scale 4 and orientation 8.

5.3. Accuracy Assessment

The results showed interclass confusion and were used to improve the classification further, curvelet co-occurrence matrix was used to provide features which were used to investigate how well the classes can be distinguished so as to reduce this confusion. These measures were used to examine the trend of class distribution compared to reference data set.

Table 5-3 shows classification of X3_A8 curvelet with 24 features, the user accuracy of the mono cropping ranges from 17.7% to 64.0% while that of mixed cropping is from 46.7% to 53.0%, this implies that mixed cropping has a narrow range of detection in this band, mono cropping has more chances of being detected than mixed cropping, 257 pixels of Sorghum is correctly classified which amounts to 17.7% user accuracy which means 17.7% of Sorghum pixel is in the classification image is Sorghum on the ground and 28.4% producer accuracy meaning approximately 28.4% of Sorghum ground truth pixels is present in the classified image. Soybeans have 411 pixels correctly classified which is 28.2% user accuracy and 28.7% producer accuracy. Maize has 93 correctly classified this is 10.1% user accuracy and 8.3% producer accuracy. Rice has 930 pixels classified correctly at 64.6% user accuracy and 60.7% producer accuracy.

Curvelet Confusion Matrix

PREDICTED CLASS	ACTUAL CLASS								
	Sorghum	Soybeans	Maize	Rice	Onions, Pepper	Sorghum, Soybeans	Soybeans, Sorghum	Row Total	User Accuracy
Sorghum	257	129	237	0	106	247	473	1449	17.7
Soybeans	17	411	56	192	652	2	126	1456	28.2
Maize	34	83	93	17	61	98	538	924	10.1
Rice	0	78	2	930	420	0	9	1439	64.6
Onions, Pepper	24	153	86	209	623	6	62	1163	53.6
Sorghum, Soybeans	29	2	72	6	53	915	535	1612	56.8
Soybeans, Sorghum	543	576	568	177	1231	1620	4124	8839	46.7
Column Total	904	1432	1114	1531	3146	2888	5867	16882	
Producer Accuracy	28.4	28.7	8.3	60.7	19.8	31.7	70.3		
Overall Accuracy									43.6

Table 5-3. Confusion matrix of SVM Classification of X3_A8_24

Curvelet Confusion Matrix

PREDICTED CLASS	ACTUAL CLASS								
	Sorghum	Soybeans	Maize	Rice	Onions, Pepper	Sorghum, Soybeans	Soybeans, Sorghum	Row Total	User Accuracy
Sorghum	425	98	441	0	76	603	852	2495	17.0
Soybeans	7	542	162	183	730	6	181	1811	29.9
Maize	28	30	138	75	39	77	537	924	14.9
Rice	0	101	10	1027	344	0	35	1517	67.7
Onions, Pepper	18	112	64	158	1189	360	131	2032	58.5
Sorghum, Soybeans	193	89	5	0	58	1318	587	2250	58.6
Soybeans, Sorghum	233	460	294	88	710	524	3544	5853	60.6
Column Total	904	1432	1114	1531	3146	2888	5867	16882	
Producer Accuracy	47.0	37.8	12.4	67.1	37.8	45.6	60.4		
Overall Accuracy									48.5

Table 5-4. Confusion matrix of SVM Classification of X3_A16_48.

Mixed cropping containing onions has user accuracy of 53.6% and producer accuracy of 19.8%. Mixed Cropping containing Sorghum as main crop and Soybeans has 915 pixels correctly classified with user accuracy of 56.8% and producer accuracy of 31.7%. Mixed Cropping containing Soybeans as main crop and Sorghum has 4124 pixels correctly classified with user accuracy of 46.7% and producer accuracy of 70.3%

The classes "Sorghum" and "Maize" are difficult to classify this means many of their test set pixels were not correctly allocated to the "Sorghum" and "Maize classes respectively, giving underestimation of the areas of these classes in the classified image. Soybeans and sorghum class proportion are more than expected due to the fact that many pixels of other classes were all counted as the soybeans and sorghum class in the classified image. The user accuracy for mono-cropping varies from 10.1% to 67.7% while that of the mixed cropping varies from 46.7% to 64.5%.

Table 5-4 shows the confusion matrix of the classification of decomposed at scale 3 and 16 orientation at the coarsest scale, it shows 425 pixels of Sorghum is correctly classified which amounts to 17.0% user accuracy which means 17.0% of Sorghum pixel is in the classification image is Sorghum on the ground and 47.0% producer accuracy meaning approximately 47.0% of Sorghum ground truth pixels is present in the classified image. Soybeans has 542 pixels correctly classified which is 29.9% user accuracy and 37.8% producer accuracy. Maize has 138 correctly classified this is 14.9% user accuracy and 12.4% producer accuracy. Rice 1027 pixel correctly 67.7% user accuracy and 67.1% producer accuracy. Mixed Cropping containing Onions and pepper has 11189 pixels correctly classified with user accuracy of 58.5% and producer accuracy of 37.8%. Mixed Cropping containing Sorghum as main crop and Soybeans has 1318 pixels correctly classified with user accuracy of 58.6% and producer accuracy of 45.6%. Mixed Cropping containing Soybeans as main crop and Sorghum has 5867 pixels correctly classified with user accuracy of 60.6% and producer accuracy of 60.4%

The result shows the similar trend as that of scale 3 orientation 8 the class "Sorghum" and "Maize" is difficult to classify because many of their test set pixels were not correctly from the "Sorghum" and "Maize classes respectively, giving underestimation of the areas of these classes in the classified image. Onion and Pepper class proportion is more than expected due to the fact that many pixels of other classes were all counted as the Onion and Pepper class in the classified image.

Curvelet Confusion Matrix									
				ACTUAL CLASS					
PREDICTED CLASS	Sorghum	Soybeans	Maize	Rice	Onions, Pepper	Sorghum, Soybeans	Soybeans, Sorghum	Row Total	User Accuracy
Sorghum	480	66	282	0	86	685	393	1992	24.1
Soybeans	8	377	93	210	700	0	151	1539	24.5
Maize	42	110	132	97	35	144	345	905	14.6
Rice	0	108	77	910	490	5	75	1665	54.7
Onions, Pepper	41	206	77	232	1066	51	84	1757	60.7
Sorghum, Soybeans	27	70	6	0	107	1516	623	2349	64.5
Soybeans, Sorghum	306	495	447	82	662	487	4196	6675	62.9
Column Total	904	1432	1114	1531	3146	2888	5867	16882	
Producer Accuracy	53.1	26.3	11.8	59.4	33.9	52.5	71.5		
Overall Accuracy									51.4

Table 5-5. Confusion matrix of SVM Classification of X4_A8_40

Curvelet Confusion Matrix									
				ACTUAL CLASS					
PREDICTED CLASS	Sorghum	Soybeans	Maize	Rice	Onions, Pepper	Sorghum, Soybeans	Soybeans, Sorghum	Row Total	User Accuracy
Sorghum	595	33	210	0	131	753	327	2049	29.0
Soybeans	21	555	128	335	787	10	619	2455	22.6
Maize	8	20	346	22	90	106	1346	1938	17.9
Rice	0	208	82	825	592	0	34	1741	47.4
Onions, Pepper	1	71	50	291	912	119	123	1567	58.2
Sorghum, Soybeans	139	115	3	0	80	1157	788	2282	50.7
Soybeans, Sorghum	140	430	295	58	554	743	2630	4850	54.2
Column Total	904	1432	1114	1531	3146	2888	5867	16882	
Producer Accuracy	65.8	38.8	31.1	53.9	29.0	40.1	44.8		
Overall Accuracy									41.6

Table 5-6. Confusion matrix of SVM Classification of X4_A16_80.

Table 5-8 shows 480 pixels of Sorghum is correctly classified which amounts to 24.1% user accuracy which means 24.1% of Sorghum pixel is in the classification image is Sorghum on the ground and 53.1% producer accuracy meaning approximately 53.1% of Sorghum ground truth pixels is present in the classified image. Soybeans has 377 pixels correctly classified which is 24.5 user accuracy and 26.3% producer accuracy. Maize has 132 pixels correctly classified this is 14.6% user accuracy and 11.8 producer accuracy. Rice 910 pixel correctly 54.7% user accuracy and 59.4% producer accuracy. Mixed Cropping containing Onions and pepper has 1066 pixels correctly classified with user accuracy of 60.7% and producer accuracy of 33.9%. Mixed Cropping containing Sorghum as main crop and Soybeans has 1516 pixels correctly classified with user accuracy of 64.5% and producer accuracy of 52.5%. Mixed Cropping containing Soybeans as main crop and Sorghum has 4196 pixels correctly classified with user accuracy of 62.9% and producer accuracy of 71.5% This trend deviates from the previous in this case the class "Sorghum" and "Soybeans" are difficult to classify because many of their test set pixels were not correctly from the "Sorghum" and "Soybeans" classes respectively, giving underestimation of the areas of these classes in the classified image. Maize class proportion is more than expected due to the fact that many pixels of other classes were all counted as the Onion and Pepper class in the classified image.

Table 5-6 shows the confusion matrix of the CCM decomposed at scale 4 and 16 orientation at the coarsest scale. It shows 595 pixels of Sorghum is correctly classified which amounts to 29.0% user accuracy which means 29.0% of Sorghum pixel is in the classification image is Sorghum on the ground and 65.8% producer accuracy meaning approximately 65.8% of Sorghum ground truth pixels is present in the classified image. Soybeans has 555 pixels correctly classified which is 22.6% user accuracy and 38.8% producer accuracy. Maize has 346 correctly classified this is 17.9% user accuracy and 31.1% producer accuracy. Rice has 825 pixels correctly classified with 47.4% user accuracy and 53.9% producer accuracy. Mixed Cropping containing Onions and pepper has 912 pixels correctly classified with user accuracy of 58.2% and producer accuracy of 29.0%. Mixed Cropping containing Sorghum as main crop and Soybeans has 1157 pixels correctly classified with user accuracy of 50.7% and producer accuracy of 40.1%. Mixed Cropping containing Soybeans as main crop and Sorghum has 2630 pixels correctly classified with user accuracy of 54.2% and producer accuracy of 44.8%

The class "Soybeans" and "Maize" are difficult to classify because many of their test set pixels were not correctly from the "Soybeans" and "Maize classes respectively, giving underestimation of the areas of these classes in the classified image. Onion and Pepper class proportion is more than expected due to the fact that many pixels of other classes were all counted as the Onion and Pepper class in the classified image.

Table 5-7 shows 571 pixels of Sorghum is correctly classified which amounts to 35.5% user accuracy which means 35.5% of Sorghum pixel is in the classification image is Sorghum on the ground and 63.2% producer accuracy meaning approximately 63.2% of Sorghum ground truth pixels is present in the classified image. Soybeans has 867 pixels correctly classified which is 28.0% user accuracy and 60.5% producer accuracy. Maize has 304 correctly classified this is 21.0% user accuracy and 27.3% producer accuracy. Rice 1240 pixel correctly 73.2% user accuracy and 27.3% producer accuracy.

Curvelet Confusion Matrix									
				ACTUAL CLASS					
PREDICTED CLASS	Sorghum	Soybeans	Maize	Rice	Onions, Pepper	Sorghum, Soybeans	Soybeans, Sorghum	Row Total	User Accuracy
Sorghum	571	52	0	0	0	334	653	1610	35.5
Soybeans	109	867	39	161	1743	40	136	3095	28.0
Maize	0	13	304	20	3	134	976	1450	21.0
Rice	0	115	155	1240	183	0	0	1693	73.2
Onions, Pepper	0	90	61	109	1124	8	440	1832	61.4
Sorghum, Soybeans	59	197	213	0	0	1257	1271	2997	41.9
Soybeans, Sorghum	165	98	342	1	93	1115	2391	4205	56.9
Column Total	904	1432	1114	1531	3146	2888	5867	16882	
Producer Accuracy	63.2	60.5	27.3	81.0	35.7	43.5	40.8		
Overall Accuracy									45.9

Table 5-7. Confusion matrix of SVM Classification of X7_A8_168.

Curvelet Confusion Matrix									
				ACTUAL CLASS					
PREDICTED CLASS	Sorghum	Soybeans	Maize	Rice	Onions, Pepper	Sorghum, Soybeans	Soybeans, Sorghum	Row Total	User Accuracy
Sorghum	605	34	290	0	106	498	192	1725	35.1
Soybeans	5	721	151	371	1016	11	517	2792	25.8
Maize	3	13	275	26	72	121	1261	1771	15.5
Rice	0	184	62	800	457	0	30	1533	52.2
Onions, Pepper	14	85	54	283	817	142	164	1559	52.4
Sorghum, Soybeans	165	136	0	0	85	1547	984	2917	53.0
Soybeans, Sorghum	112	259	282	51	593	569	2719	4585	59.3
Column Total	904	1432	1114	1531	3146	2888	5867	16882	
Producer Accuracy	66.9	50.3	24.7	52.3	26.0	53.6	46.3		
Overall Accuracy									44.3

Table 5-8. Confusion matrix of SVM Classification of Combine X3_A8, X3_A16, X4_A8, X4_A16

Mixed Cropping containing Onions and pepper has 1124 pixels correctly classified with user accuracy of 61.4% and producer accuracy of 37.5%. Mixed Cropping containing Sorghum as main crop and Soybeans has 1257 pixels correctly classified with user accuracy of 41.9% and producer accuracy of 43.5%. Mixed Cropping containing Soybeans as main crop and Sorghum has 2391 pixels correctly classified with user accuracy of 56.9% and producer accuracy of 40.8%

The classes "Sorghum" and "Maize" are difficult to classify because many of their test set pixels were not correctly from the "Sorghum" and "Maize classes respectively, giving underestimation of the areas of these classes in the classified image. Onion and Pepper class proportion is more than expected due to the fact that many pixels of other classes were all counted as the Onion and Pepper class in the classified image.

Table 5-7 show the result of combining decomposition at scale 3 and 4 using orientations 8 and 16 the result shows that 605 pixels of Sorghum is correctly classified which amounts to 35.1% user accuracy which means 35.1% of Sorghum pixel is in the classification image is Sorghum on the ground and 66.9% producer accuracy meaning approximately 66.9% of Sorghum ground truth pixels is present in the classified image. Soybeans has 721% pixels correctly classified which is 25.8% user accuracy and 50.5 producer accuracy. Maize has 275 pixels correctly classified this is 15.5% user accuracy and 24.7 producer accuracy. Rice 800 pixel correctly 52.2% user accuracy and 52.5% producer accuracy.

Mixed Cropping containing Onions and pepper has 817 pixels correctly classified with user accuracy of 52.4% and producer accuracy of 26.0%. Mixed Cropping containing Sorghum as main crop and Soybeans has 784 pixels correctly classified with user accuracy of 53.0% and producer accuracy of 53.6%. Mixed Cropping containing Soybeans as main crop and Sorghum has 4057 pixels correctly classified with user accuracy of 59.3% and producer accuracy of 46.3%

The classes "Sorghum" and "Maize" are difficult to classify because many of their test set pixels were not correctly from the "Sorghum" and "Maize classes respectively, giving underestimation of the areas of these classes in the classified image. Onion and Pepper class proportion is more than expected due to the fact that many pixels of other classes were all counted as the Onion and Pepper class in the classified image.

After examining the the confusion matrix of the classification, all elements of scale X3 and X4 where added together and linear SVM classification was done. This is done to improve overall accuracy of detection. The result obtained was lower than that of the single decomposition scale (Figure 5-7). The combination of the two scale increases the feature space hence the classification was computationally more intensive than when scale X3 or X4 was used alone.

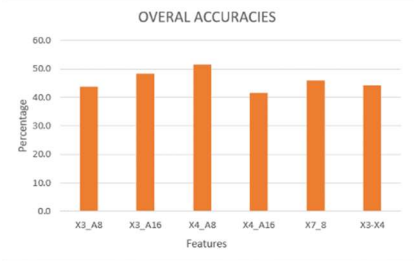

Figure 5-7. Overall accuracy of scale X3 to X4 and combined X3 and X4

FEATURE	Overall Accuracy at cost 10	Contingency measures at cost 10
X2_A8	40.1	42.4
X2_A16	40.6	49.2
X3_A8	43.6	57.9
X3_A16	48.5	78.5
X4_A8	51.4	75.7
X4_A16	41.6	95.6
X5_A8	45.1	93.8
X5_A16	44.2	100.0
X6_A8	41.9	100.0
X6_A16	50.0	100.0
X7_A8	45.9	100.0

Table 5-9. Overall Accuracy and Contingency Analysis at different decomposition scales and orientation

Table 5-9 shows the contingency analysis at cost 10 of all scales and the overall accuracies. This shows that as the number of features increases the sereparability increases. After comparing the trend of contingency analysis and the overall accuracies, a further test was carried out for ascertaining the overall accuracy of the cropping system. This test is done to see the performance of the classifier in detecting only either mono cropping or mixed cropping without knowing what is planted on the field. The result of using the two classes in the classifier is presented in the subsequent paragraphs.

The result of classifying the cropping system using two classes, mono cropping and mixed cropping is shown in

Table 5-10. The classifier did not distinguish the cropping system at scale X2. The distinction of the cropping system has highest accuracy of 70% at scale XA_A8. The lowest accuracy is 59.4%, it is obtained at X6_A16. This shows that the detection of mixed cropping is higher than that of mono-cropping at XA_A8 The accuracies did not follow a linear relationship with increase in scale. Looking at

FEATURE	COST 10
X3_A8	70.0
X3_A16	66.5
X4_A8	69.1
X4_A16	67.8
X5_A8	66.4
X5_A16	65.9
X6_A8	68.1
X6_A16	59.4
X7_A8	64.1

Table 5-10. Accuracy of detecting mono cropping and mixed cropping.

From the classification map of Figure 5-8. Mono cropping and mixed cropping classification the classification of X3_A8 really modelled the farm. The crop fields are better separated compare to the other maps, the distinction between the mono cropping fields and mixed cropping fields is not as noisy as other maps. Map of X3_A8 (Figure 5-8) also produces a better visual distinction of the cropping system than map of other scales.

X3_A8		ACTUAL CLASS			
		Mono	Mixed	Row Sum	User Accuracy
PREDICTED CLASS	Mono	2852	2935	5787	49.3
	Mixed	2129	8966	11095	26.5
	Column Total	4981	11901	16882	
	Producer Accuracy	57.3	32.7		
	Overall Accuracy				70.0

Table 5-11 Confusion matrix of mono cropping and mixed cropping at X3_A8

X4_X8		ACTUAL CLASS			
		Mono	Mixed	Row Sum	User Accuracy
PREDICTED CLASS	Mono	2985	3434	6419	46.5
	Mixed	1996	8467	10463	32.8
	Column Total	4981	11901	16882	
	Producer Accuracy	59.9	40.6		
	Overall Accuracy				67.8

Table 5-12. Confusion matrix of mono cropping and mixed cropping X4_A8

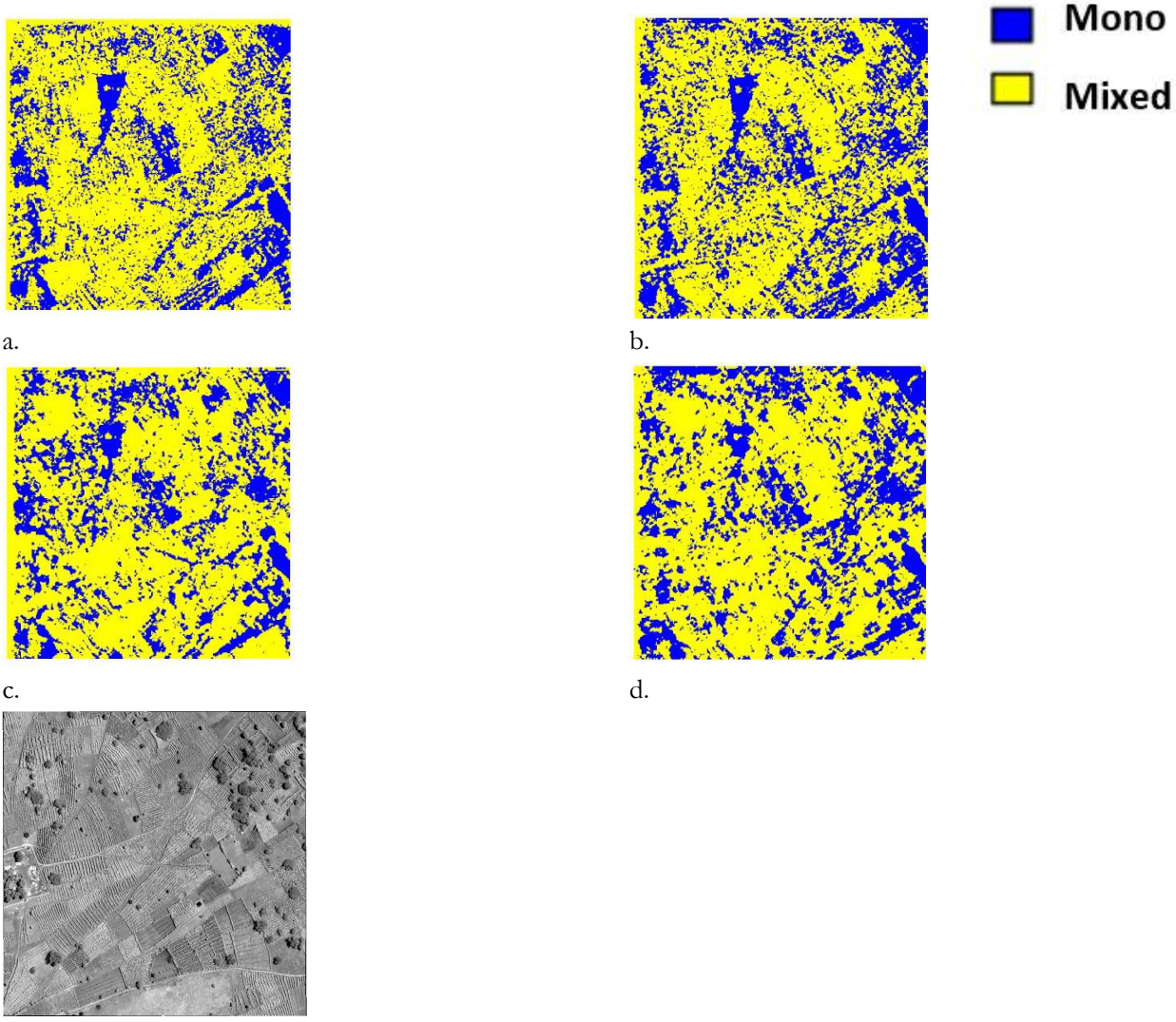

a. b.

c. d.

e.

Figure 5-8. Mono cropping and mixed cropping classification a, X3_A8 b, X3_A16 c, X4_A8 d, X4_A16 and e, panchromatic image respectively.

6. DISCUSSION

6.1. Curvelet Feature Extraction and Classification

The result of curvelet coefficient agrees with the work of Kingsbury (2006) the coefficients are symmetric, they give similar frequency response at certain orientations. The issue of spatial resolution as identified earlier by Debats et al. (2016) has been addressed by use of different scales of curvelet. Likewise, the spectral similarity of the crops has been solved by the curvelet transform by providing addition variety of features using different orientation and scales using just one panchromatic image. Rotational invariance is addressed by taking all the orientation in a particular scale.

The result obtained from the use of Daubechies wavelets is similar to that of Arivazhagan et al. (2006) showing that curvelet transforms performed better in detecting feature than when non-directional wavelet is used. Unlike the work of work of Lucieer & Van Der Werff (2007), Daubechies is not useful due to the orientation of the crop rows. Unlike the work of Kiani, Azimifar, & Kamgar (2010 who used Daubechies wavelet transform, detecting corn (maize) has lots of misclassification errors.

The Daubechies has 4 orientations at each decomposition while the curvelet has many orientations this makes curvelet better than Daubechies in detecting mono cropping and mixed cropping. This is because similar crops are planted in a different orientation. At the highest level, many more features are present than at the coarsest level, this makes it possible to get more features for distinguishing cropping system. The computed co-occurrence matrix has poor performance than the curvelet except for the mean which is slightly higher.

The use of SVM linear kernel with parameters cost set to one provided not too much desired result likewise when the cost was set to 10 however at this cost the performance is better than when cost is set to 100. This means at 100 the model is being over fitted. The optimal parameter for the linear kernel is not determined due to fixing the cost at those arbitrary values, the performance can be improved by tuning the cost parameter. This performance is also seen when RBF kernel is used, RBF is expected to perform better than linear kernel but the reverse is the case this is likely due to not turning the cost and gamma for the RBF.

6.2. Accuracy Assessment

Comparing the result of this thesis work with Lahajnar & Kovačič (2003) an improved result on the accuracy is achieved by avoiding overlapping of sample points, due to the complexity in the nature of the fields using different training set and test set at different crop orientations cannot be achieved for all crops. The result of the experiment carried out differ from the work of Han & Ma (2007) the overall accuracy and decomposition scale are not directly proportional. The reason for this is the choice of training and test set, however, the contingency analysis increases with scale. The overall accuracy of detecting mixed cropping is higher than that of detecting mono-cropping.

The result shows lower accuracy results; this could be as a result of noise because of weed that is present in the farmland. The use of curvelet in distinguishing the mono cropping and mixed cropping is difficult to achieve without factoring in the presence of weed in the farmland. This is because a field with mono-cropped field will be classified as mixed due to variety in the texture because of the presence of weed.

7. CONCLUSION AND RECOMMENDATIONS

The accuracies for detecting single crops and crop combinations ranges between 40% and 51% while the accuracy of separating mono-cropping from multiple cropping is 70%. The use of curvelet transforms performance does not vary proportionally according to scale in detecting the cropping system. The combination of co-occurrence matrix with the curvelet co-occurrence matrix does not give an overall better performance. The linear kernel performs better than RBF using fixed cost value of 10. The kernel parameters were not tuned, so the optimal performance of the kernels is not determined. The linear kernel performed better when the cost is set to 1 and also at 10 than when it was set to 100. The overall accuracy does not well represent the deferent classifications; the user accuracies give a better description of the detection when we need to know the crop type in mono-cropping and the crop types that are mixed. The overall accuracy is suitable if the classes are just split into two classes of mono cropping and mixed cropping.

Further research should be done on methods to reduce the effect of noise caused by curvelet transform as it relates to remote sensing image. It is recommended to explore the use of different kernels with a view of improving crop detection as well as investigate the effect of combining different machine learning algorithm to improve crop detection with curvelet transform.

LIST OF REFERENCES

Akar, Ö., & Güngör, O. (2015). Integrating multiple texture methods and NDVI to the random forest classification algorithm to detect tea and hazelnut plantation areas in northeast Turkey. *International Journal of Remote Sensing*, *36*(2), 442–464. http://doi.org/10.1080/01431161.2014.995276

Akhtar, A., Nazir, M., & Khan, S. A. (2012). Crop classification using feature extraction from satellite imagery. In *2012 15th International Multitopic Conference (INMIC)* (pp. 9–15). Islamabad: IEEE. http://doi.org/10.1109/INMIC.2012.6511479

Arivazhagan, S., & Ganesan, L. (2003). Texture segmentation using wavelet transform. *Pattern Recognition Letters*, *24*(16), 3197–3203. http://doi.org/10.1016/j.patrec.2003.08.005

Arivazhagan, S., Ganesan, L., & Kumar, S. T. G. (2006). Texture classification using curvelet statistical and co-occurrence Features. *Proceedings - International Conference on Pattern Recognition*, *2*, 938–941. http://doi.org/10.1109/ICPR.2006.1110

Bovik, A. C., Clark, M., & Geisler, W. S. (1990). Multichannel texture analysis using localized spatial Filters. *IEEE Transactions on Pattern Analysis and Machine Intelligence*, *12*(1), 55–73. http://doi.org/10.1109/34.41384

Campbell, J. B., & Wynne, R. H. (2011). *Introduction to remote sensing*. New York: Guilford Press.

Candès, E. J., Demanet, L., Donoho, D., & Ying, L. (2006). Fast discrete curvelet transforms. *Multiscale Modeling & Simulation*, *5*(3), 861–899. http://doi.org/10.1137/05064182X

Canters, F. (1997). Evaluating the Uncertainty of Area Estimates Derived from Fuuy Land-Cover Classification. *Photogrammetric Engineering & Remote Sensing*, *63*(4), 403–414.

Cavusoglu, B. (2014). Multiscale texture retrieval based on low-dimensional and rotation-invariant features of curvelet transform. *EURASIP Journal on Image and Video Processing*, *2014*(1), 22. http://doi.org/10.1186/1687-5281-2014-22

Chen, Z., Wang, L., Wu, W., Jiang, Z., & Li, H. (2016). Monitoring Plastic-Mulched Farmland by Landsat-8 OLI Imagery Using Spectral and Textural Features. *Remote Sensing*, *8*(4), 353. http://doi.org/10.3390/rs8040353

Christensen, K. (2015). *Maize--Legume intercropping 2014 phase 1 and 2 trial report*. Retrieved from www.oneacrefund.org

Congalton, R. G., & Green, K. (2009). *Assessing the Accuracy of Remotely Sensed Data: Principles and Practices*. (2nd, Ed.) (Vol. null).

Crane, R. (1997). *A simplified approach to image processing□ : Classical and modern techniques in C*. Prentice Hall PTR.

Curvelab. (2016). Curvelet software. CurveLab Toolbox, Version 2.1.3. Retrieved October 27, 2016, from http://curvelet.org/software.html

Daubechies, I. (1992). *Ten lectures on wavelets*. SIAM. http://doi.org/http://dx.doi.org/10.1137/1.9781611970104

Debats, S. R., Luo, D., Estes, L. D., Fuchs, T. J., & Caylor, K. K. (2016). A generalized computer vision approach to mapping crop fields in heterogeneous agricultural landscapes. *Remote Sensing of Environment*, *179*, 210–221. http://doi.org/10.1016/j.rse.2016.03.010

DeFries, R. S., & Los, S. O. (1999). Implications of land-cover misclassification for parameter estimates in global land-surface models: an example from the simple biosphere model (SiB2). *Photogrammetric Engineering and Remote Sensing*, *65*(9), 1083–1088. Retrieved from http://cat.inist.fr/?aModele=afficheN&cpsidt=1961019

Dettori, L., & Semler, L. (2007). A comparison of wavelet, ridgelet, and curvelet-based texture classification algorithms in computed tomography. *Computers in Biology and Medicine*, *37*(4), 486–498. http://doi.org/10.1016/j.compbiomed.2006.08.002

Dong, Y., Wang, J., Li, C., Yang, G., Xu, X., Zhao, J., & Huang, W. (2012). Integration of multi-resolution data for crop LAI estimation based on continuous wavelet. In *2012 IEEE International Geoscience and Remote Sensing Symposium* (pp. 6665–6668). IEEE. http://doi.org/10.1109/IGARSS.2012.6352070

Duguma, B., Gockowski, J., & Bakala, J. (2001). Smallholder cacao (Theobroma cacao Linn.) cultivation in agroforestry systems of West and Central Africa: Challenges and opportunities. *Agroforestry Systems*. Retrieved from http://link.springer.com/article/10.1023/A:1010747224249

Elhabiby, M., Elsharkawy, A., & El-sheimy, N. (2012). Second generation curvelet transforms vs wavelet transforms and canny edge detector foredge detection from WorldView-2 data. *International Journal of Computer Science and Engineering Surve*, *3*(4), 1–13.

Foody, G. M. (2002). Status of land cover classification accuracy assessment. *Remote Sensing of Environment*, *80*(1), 185–201. http://doi.org/10.1016/S0034-4257(01)00295-4

Francis, C. (1989). Biological efficiencies in multiple-cropping systems. *Advances in Agronomy*. Retrieved from http://www.sciencedirect.com/science/article/pii/S0065211308605222

Gómez, F., & Romero, E. (2011). Rotation invariant texture characterization using a curvelet based descriptor. *Pattern Recognition Letters*, *32*(16), 2178–2186. http://doi.org/10.1016/j.patrec.2011.09.029

Han, J., & Ma, K.-K. (2007). Rotation-invariant and scale-invariant Gabor features for texture image retrieval. *Image and Vision Computing*, *25*(9), 1474–1481. http://doi.org/10.1016/j.imavis.2006.12.015

Haralick, R. M. (1979). Statistical and structural approaches to texture. *Proceedings of the IEEE*, *67*(5), 786–804. http://doi.org/10.1109/PROC.1979.11328

Hassan, A., Riaz, F., & Shaukat, A. (2014). Scale and rotation invariant texture classification using covariate shift methodology. *IEEE Signal Processing Letters*, *21*(3), 321–324. http://doi.org/10.1109/LSP.2014.2302576

Haykin, S. (2001). Adaptive systems for signal process. In Stergios Stergiopoulos (Ed.), *Advanced Signal Processing Handbook*. CRC Press LLC.

Islam, M. M., Zhang, D., & Lu, G. (2009). Rotation invariant curvelet features for texture image retrieval. *2009 IEEE International Conference on Multimedia and Expo*, *1*(c), 562–565. http://doi.org/10.1109/ICME.2009.5202558

Jafari-Khouzani, K., & Soltanian-Zadeh, H. (2005). Radon transform orientation estimation for rotation invariant texture analysis. *IEEE Transactions on Pattern Analysis and Machine Intelligence*, *27*(6), 1004–1008. http://doi.org/10.1109/TPAMI.2005.126

Jähne, B. (2002). Image Representation. In *Digital Image Processing* (5th ed., pp. 29–76). Berlin, Heidelberg: Springer Berlin Heidelberg. http://doi.org/10.1007/978-3-662-04781-1_2

Kaur, M., & Pooja. (2015). Wavelet and curvelet transformation based image fusion with ANFIS and SVM. *International Journal of Computer Applications*, *121*(14), 13–19.

Kingsbury, N. (2006). Rotation-invariant local feature matching with complex wavelets. *European Signal Processing Conference*, (44), 4–8.

Kumar, D. A., & Prema, P. (2015a). A novel wrapping curvelet transformation based angular texture pattern (wctatp) extraction method for weed identification. *ICTACT Journal on Image and Video Processing*, 1192–1206.

Kumar, D. A., & Prema, P. (2015b). A study on weed discrimination through wavelet transform, texture feature extraction and classification. *International Journal of Computer Science and Information Technology*, *7*(3), 41–52. http://doi.org/10.5121/ijcsit.2015.7304

Lahajnar, F., & Kovačič, S. (2003). Rotation-invariant texture classification. *Pattern Recognition Letters*, *24*(9), 1151–1161. http://doi.org/10.1016/S0167-8655(02)00285-4

Li, L., Sun, J., Zhang, F., Li, X., Yang, S., & Rengel, Z. (2001). Wheat/maize or wheat/soybean strip intercropping I. Yield advantage and interspecific interactions on nutrients. *Field Crops Research*, *71*(2), 123–137. http://doi.org/10.1016/S0378-4290(01)00156-3

Li, S., & Shawe-Taylor, J. (2005). Comparison and fusion of multiresolution features for texture classification. *Pattern Recognition Letters*, *26*(5), 633–638. http://doi.org/10.1016/j.patrec.2004.09.013

Liang, Y., Gong, W., Pan, Y., Li, W., & Hu, Z. (2005). Gabor features-based classification using SVM for face recognition (pp. 118–123). http://doi.org/10.1007/11427445_20

Livens, S., Scheunders, P., Van de Wouwer, G., Van Dyck, D., Smets, H., Winkelmans, J., & Bogaerts, W. (1996). A texture analysis approach to corrosion image classification. *Microscopy Microanalysis Microstructures*, *7*(2), 143–152. http://doi.org/10.1051/mmm:1996110

Livens, S., Scheunders, P., Wouwer, G. Van de, & Dyck, D. Van. (1997). Wavelets for texture analysis. *International Journal of Computing Science and Mathematics*, 1–5. http://doi.org/10.1.1.27.3263

Lu, D., & Weng, Q. (2007). A survey of image classification methods and techniques for improving classification performance. *International Journal of Remote Sensing*, *28*(5), 823–870. http://doi.org/10.1080/01431160600746456

Lucieer, A., & Van Der Werff, H. (2007). Panchromatic wavelet texture features fused with multispectral bands for improved classification of high-resolution satellite imagery. *International Geoscience and Remote Sensing Symposium (IGARSS)*, *2*, 5154–5157. http://doi.org/10.1109/IGARSS.2007.4424022

Manthalkar, R., Biswas, P. K., & Chatterji, B. N. (2003). Rotation invariant texture classification using even symmetric Gabor filters. *Pattern Recognition Letters*, *24*(12), 2061–2068. http://doi.org/10.1016/S0167-8655(03)00043-6

Marques, J. P. (2001). *Pattern Recognition: Concepts, Methods and Applications*. Berlin, Heidelberg: Springer Berlin Heidelberg. http://doi.org/10.1007/978-3-642-56651-6

Meyer, D., Dimitriadou, E., Hornik, K., Weingessel, A., & Leisch, F. (2015). e1071: Misc functions of the department of statistics, probability theory group (formerly: E1071), TU Wien. Retrieved from https://cran.r-project.org/package=e1071

Nixon, M., & Aguado, A. S. (2012). Introduction to texture description, segmentation, and classification. In *Feature Extraction & Image Processing for Computer Vision* (pp. 399–434). http://doi.org/10.1016/B978-0-12-396549-3.00008-2

Okigbo, B., & Greenland, D. (1976). Intercropping systems in tropical Africa. *International Institute of Tropical Agriculture, Sd.* Retrieved from http://libcatalog.cimmyt.org/download/reprints/94276.pdf

Patil, A., & Lalitha, Y. S. (2015). Crop species identification using NN tool. *Esatjournals.net*, 1–6. Retrieved from http://esatjournals.net/ijret/2015v04/i17/IJRET20150417023.pdf

Peña-Barragán, J. M., Ngugi, M. K., Plant, R. E., & Six, J. (2011). Object-based crop identification using multiple vegetation indices, textural features and crop phenology. *Remote Sensing of Environment*, *115*(6), 1301–1316. http://doi.org/10.1016/j.rse.2011.01.009

Pontius, R. G., & Millones, M. (2011). Death to Kappa: birth of quantity disagreement and allocation disagreement for accuracy assessment. *International Journal of Remote Sensing*, *32*(15), 4407–4429. http://doi.org/10.1080/01431161.2011.552923

Prema, P., & Murugan, D. (2016). A Novel Angular Texture Pattern (ATP) Extraction Method for Crop and Weed Discrimination Using Curvelet Transformation, *15*(1), 27–59.

Pujari, J. D., Yakkundimath, R., & Byadgi, A. S. (2016). SVM and ANN based classification of plant diseases using feature reduction technique. *International Journal of Interactive Multimedia and Artificial Intelligence*, *3*(7), 6. http://doi.org/10.9781/ijimai.2016.371

R Core Team. (2016). R: A language and environment for statistical computing. Vienna, Austria. Retrieved from https://www.r-project.org/

Riaz, F., Silva, F. B., Ribeiro, M. D., & Coimbra, M. T. (2012). Invariant Gabor Texture Descriptors for Classification of Gastroenterology Images. *IEEE Transactions on Biomedical Engineering*, *59*(10), 2893–2904. http://doi.org/10.1109/TBME.2012.2212440

Richards, J. A. (2013). *Remote Sensing Digital Image Analysis. Methods* (5th ed.). Berlin, Heidelberg: Springer Berlin Heidelberg. http://doi.org/10.1007/978-3-642-30062-2

Rokni, K., Ahmad, A., Solaimani, K., & Hazini, S. (2015). A new approach for surface water change detection: Integration of pixel level image fusion and image classification techniques. *International Journal of Applied Earth Observation and Geoinformation*, *34*, 226–234. http://doi.org/10.1016/j.jag.2014.08.014

Serrano, Á., de Diego, I. M., Conde, C., & Cabello, E. (2010). Recent advances in face biometrics with gabor wavelets: A review. *Pattern Recognition Letters*, *31*(5), 372–381. http://doi.org/10.1016/j.patrec.2009.11.002

Shapiro, L. G., & Stockman, G. C. (2001). *Computer vision*. New Jersey: Prentice Hall.

Shen, L., & Ji, Z. (2009). Gabor wavelet selection and SVM classification for object recognition. *Acta Automatica Sinica*, *35*(4), 350–355. http://doi.org/10.1016/S1874-1029(08)60082-8

Shen, L., & Yin, Q. (2007). Texture Classification Using Curvelet Transform. *International Journal of Wavelets, Multiresolution and Information Processing*, *5*(3), 451–464. http://doi.org/10.1142/S0219691307001847

Stoop, W. (1986). Agronomic management of cereal/cowpea cropping systems for major toposequence land types in the West African sacanna. *Field Crops Research*. Retrieved from http://www.sciencedirect.com/science/article/pii/0378429086900663

Stoop, W. (1987). Adaptation of sorghum/maize and sorghum/pearl millet intercrop systems to the toposequence land types in the North Sudanian zone of the west African Savanna. *Field Crops Research*, *16*(3), 255–272. http://doi.org/10.1016/0378-4290(87)90064-5

Sumana, I. J., Lu, G., & Zhang, D. (2012). Comparison of curvelet and wavelet texture features for content based image retrieval. *Proceedings - IEEE International Conference on Multimedia and Expo*, 290–295. http://doi.org/10.1109/ICME.2012.90

Tso, B., & Mather, P. M. . (2009). Methods based on fuzzy set theory. In *Classification Methods for Remotely Sensed Data* (Second, pp. 155–181). CRC press Boca Raton.

UNSD. (2016). United Nations Statistics Division - Environment Statistics. Retrieved June 2, 2016, from http://unstats.un.org/unsd/environmentgl/gesform.asp?getitem=761

Vo, A., & Oraintara, S. (2010). A study of relative phase in complex wavelet domain: Property, statistics and applications in texture image retrieval and segmentation. *Signal Processing: Image Communication*, *25*(1), 28–46. http://doi.org/10.1016/j.image.2009.09.003

Zhang, D., Islam, M. M., Lu, G., & Sumana, I. J. (2012). Rotation invariant curvelet features for region based image retrieval. *International Journal of Computer Vision*, *98*(2), 187–201. http://doi.org/10.1007/s11263-011-0503-6

Zhang, F., & Li, L. (2003). Using competitive and facilitative interactions in intercropping systems enhances crop productivity and nutrient-use efficiency. *Plant and Soil*, *248*(1/2), 305–312. http://doi.org/10.1023/A:1022352229863

Zhi, L., Guizhong, L., Yang, Y., & Junyong, Y. (2012). Scale- and rotation-invariant local binary pattern using scale-adaptive texton and subuniform-based circular shift. *IEEE Transactions on Image Processing*, *21*(4), 2130–2140. http://doi.org/10.1109/TIP.2011.2173697

Zou, J., Liu, C.-C., Zhang, Y., & Lu, G.-F. (2013). Object recognition using gabor co-occurrence similarity. *Pattern Recognition*, *46*(1), 434–448. http://doi.org/10.1016/j.patcog.2012.06.018